Finite Differences and Finite Elements in Nonlocal Fracture Modeling: A Priori Convergence Rates

Prashant K. Jha and Robert Lipton

Contents

Abstract

In this chapter we present a rigorous convergence analysis of finite difference and finite element approximation of nonlinear nonlocal models. In the previous chapter, we considered a differentiable version of the original bond-based model introduced in Silling (J Mech Phys Solids 48(1):175–209, 2000). There we showed, for a fixed horizon of nonlocal interaction ϵ, that well-posed formulations of the model can be developed over Hölder spaces and Sobolev

P. K. Jha
Department of Mathematics, Louisiana State University, Baton Rouge, LA, USA
e-mail: prashant.j16o@gmail.com; jha@math.lsu.edu

R. Lipton (✉)
Department of Mathematics, and Center for Computation and Technology, Louisiana State University, Baton Rouge, LA, USA
e-mail: lipton@math.lsu.edu; lipton@lsu.edu

© Springer International Publishing AG 2018
G. Z. Voyiadjis (ed.), *Handbook of Nonlocal Continuum Mechanics for Materials and Structures*, https://doi.org/10.1007/978-3-319-22977-5_44-1

spaces. In this chapter we apply these formulations to show a priori convergence for the discrete finite difference and finite element methods. We show that the error made using the forward Euler in time and a finite difference (i.e., piecewise constant) discretization in space with time step Δt and spatial discretization h is of the order of $O(\Delta t + h/\epsilon^2)$. For a central difference approximation in time and piecewise linear finite element approximation in space, the approximation error is of the order of $O(\Delta t + h^2/\epsilon^2)$. We point out these are the first such error estimates for nonlinear nonlocal fracture formulations and are reported in Jha and Lipton (2017b Numerical analysis of nonlocal fracture models models in holder space. arXiv preprint arXiv:1701.02818. To appear in SIAM Journal on Numerical Analysis 2018) and Jha and Lipton (2017a, Finite element approximation of nonlocal fracture models. arXiv preprint arXiv:1710.07661). We then go on to prove the stability of the semi-discrete approximation and show that the energy of the discrete approximation is bounded in terms of work done by the body force and initial energy put into the system. We look forward to improvements and development of a posteriori error estimation in the coming years.

Keywords

Peridynamic modeling · Finite differences · Finite elements · Stability · Convergence

Introduction

In this chapter we present a rigorous convergence analysis of finite difference and finite element approximation of nonlinear nonlocal fracture models. The model considered in this work is a differentiable version of the original peridynamic bond-based model introduced in Silling (2000) and analyzed in Lipton (2014, 2016). It is a bond-based model characterized by a nonlinear double-well potential. As discussed in the previous chapter, the nonlocal evolution converges to a sharp fracture evolution with bounded Griffith fracture energy as the length scale of nonlocality ϵ tends to zero. In this limit the displacement field satisfies the linear elastic wave equation off the fracture set.

We first consider the forward Euler time discretization and finite difference approximations in space with a uniform square mesh in 2-d and cubic mesh in 3-d. The mesh size is taken to be h and the time step is Δt. An a priori bound on the error is obtained for solutions in the Hölder space $C_0^{0,\gamma}(D;\mathbb{R}^d)$, where $\gamma \in (0,1]$ is the Hölder exponent, D is the material domain, and $d = 2, 3$ is the dimension. The rate of convergence is shown to be no larger than $O(\Delta t + h^\gamma/\epsilon^2)$. We also show stability of the semi-discrete approximation. The semi-discrete evolution is shown to be uniformly bounded in time in terms of initial energy and the work done by body force. In this chapter we prove all results for the forward Euler in time discretization, and we refer to Jha and Lipton (2017b) for the general single-step time discretization.

Next we consider central differences in time and a finite element discretization in space using triangular or tetrahedral meshes and conforming linear elements. Assuming $H_0^2(D;\mathbb{R}^d)$ solutions, we estimate the error and obtain a convergence rate of $O(\Delta t + h^2/\epsilon^2)$. We show that the semi-discrete evolution for the finite element scheme is also stable in time. We provide a stability analysis of the fully discrete problem, for the linearized peridynamic force. For this case we exhibit a CFL-like stability condition for the time step Δt.

The results presented here show that convergence requires $h^\gamma < \epsilon^2$ for the finite difference case while $h^2 < \epsilon^2$ (or $h < \epsilon$) for the finite element case. The technical reason for the appearance of the factor $1/\epsilon^2$ in these convergence rates is that we are numerically approximating a nonlinear but Lipschitz continuous vector valued ODE. Here the vector space is the space of square integrable displacement fields, and the $1/\epsilon^2$ factor is proportional to the Lipschitz constant of the nonlocal nonlinear force acting on mean square integrable displacement fields. Our results requiring $h < \epsilon$ are consistent with the earlier work of Tian and Du (2014) for linear nonlocal forces and finite element approximations applied to equilibrium problems. We point out that the nonlocal nonlinear models treated here are identified with sharp fracture evolutions as $\epsilon \to 0$ (see Lipton 2014, 2016). However a convergence rate with respect to ϵ remains to be established. We discuss this aspect in the conclusions section.

There is a rapidly growing literature in peridynamic modeling and analysis (see, e.g., Emmrich et al. 2007; Du and Zhou 2011; Foster et al. 2011; Aksoylu and Parks 2011; Du et al. 2013a; Dayal 2017; Emmrich et al. 2013; Mengesha and Du 2013; Lipton 2014, 2016; Lipton et al. 2016; Emmrich and Puhst 2016; Du, Tao, and Tian 2017; Lipton et al. 2018; Aksoylu and Mengesha 2010; Mengesha and Du 2013, 2014; Aksoylu and Unlu 2014). In Macek and Silling (2007), Gerstle et al. (2007), Littlewood (2010), the finite element method is applied to the peridynamics formulation for the simulation of cracks. In Du et al. (2013b), the finite element approximation of linear peridynamic models for general quasistatic evolutions is analyzed. For linear elastic local models, the stability of the general Newmark time discretization is shown in Baker (1976), Grote and Schötzau (2009), and Karaa (2012). This behavior is shown to persist for elastic nonlocal models in Guan and Gunzburger (2015). In Chen and Gunzburger (2011), the finite element approximation with continuous and discontinuous elements is developed for nonlocal problems in one dimension. A numerical analysis of linear peridynamics models for a 1-d bar has been carried out in Weckner and Emmrich (2005) and Bobaru et al. (2009). In Tian and Du (2014) and Tian et al. (2016a,b), an asymptotically compatible approximation scheme is identified. In Askari et al. (2008), Silling et al. (2010), Ha and Bobaru (2011), Agwai et al. (2011), Bobaru and Hu (2012), and Zhang et al. (2016), crack prediction and crack branching phenomenon are analyzed through peridynamics. The list of references is by no means complete; additional references to the literature can be found in this handbook.

Review of the Nonlocal Model

We define the strain associated with the displacement field $\boldsymbol{u}(x)$ as

$$S(\boldsymbol{u}) = S(y, x; \boldsymbol{u}) = \frac{\boldsymbol{u}(y) - \boldsymbol{u}(x)}{|y-x|} \cdot e_{y-x} \text{ and } e_{y-x} = \frac{y-x}{|y-x|}. \quad (1)$$

We consider the following type of potential (see Figs. 1 and 2)

$$W^\epsilon(S, y-x) = \omega(x)\omega(y)\frac{J^\epsilon(|y-x|)}{\epsilon} f(|y-x|S^2), \quad (2)$$

where the function $f : \mathbb{R}^+ \to \mathbb{R}$ is positive, smooth, and concave and satisfies the following properties

$$\lim_{r\to 0+} \frac{f(r)}{r} = f'(0), \qquad \lim_{r\to\infty} f(r) = f_\infty < \infty. \quad (3)$$

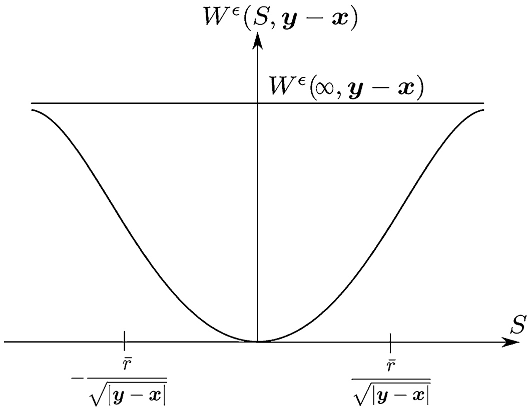

Fig. 1 Two-point potential $W^\epsilon(S, y-x)$ as a function of strain S for fixed $y-x$

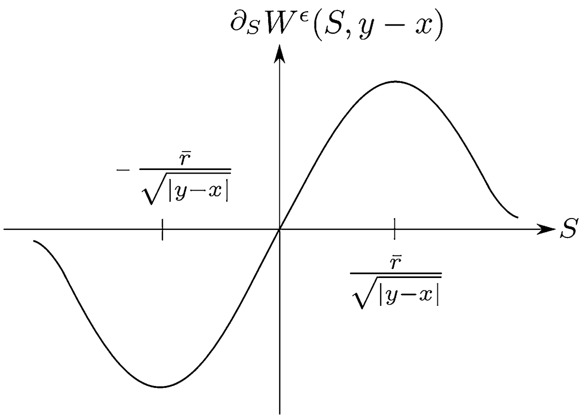

Fig. 2 Nonlocal force $\partial_S W^\epsilon(S, y-x)$ as a function of strain S for fixed $y-x$. Second derivative of $W^\epsilon(S, y-x)$ is zero at $\pm\bar{r}/\sqrt{|y-x|}$

The function $J^\epsilon(r) = J(r/\epsilon)$ is the influence function where $0 \leq J(|x|) \leq M$ for $x \in H_1(0)$ and $J = 0$ outside. The boundary function $0 \leq \omega(x) \leq 1$ takes the value 0 on the boundary ∂D of the material domain D. For $x \in D$, a distance ϵ away from boundary, $\omega(x)$ is 1 and smoothly decreases from 1 to zero as x approaches ∂D.

In the sequel we will set

$$\bar{\omega}(x) = \omega(x)\omega(x + \epsilon\xi) \tag{4}$$

and we assume

$$|\nabla\bar{\omega}| \leq C_{\omega_1} < \infty \quad \text{and} \quad |\nabla^2\bar{\omega}| \leq C_{\omega_2} < \infty.$$

The peridynamic force is written $-\nabla PD^\epsilon$ and given by

$$\begin{aligned} &-\nabla PD^\epsilon(\boldsymbol{u})(x) \\ &= \frac{2}{\epsilon^d \omega_d} \int_{H_\epsilon(x)} \partial_S W^\epsilon(S, y-x) \frac{y-x}{|y-x|} dy \\ &= \frac{4}{\epsilon^{d+1}\omega_d} \int_{H_\epsilon(x)} \omega(x)\omega(y) J^\epsilon(|y-x|) f'(|y-x|S(\boldsymbol{u})^2) S(\boldsymbol{u}) e_{y-x} dy, \end{aligned} \tag{5}$$

Peridynamics Equation

Let $u : [0, T] \times D \to \mathbb{R}^d$ be the displacement field such that it satisfies the following evolution equation

$$\rho\partial_{tt}^2 \boldsymbol{u}(t, x) = -\nabla PD^\epsilon(\boldsymbol{u}(t))(x) + b(t, x), \tag{6}$$

where $b(t, x)$ is the body force and ρ is the density. We will assume $\rho = 1$ throughout the chapter. The initial condition is given by

$$\boldsymbol{u}(0, x) = \boldsymbol{u}_0(x) \qquad \text{and} \qquad \partial_t \boldsymbol{u}(0, x) = \boldsymbol{v}_0(x) \tag{7}$$

and the boundary condition is given by

$$\boldsymbol{u}(t, x) = 0 \qquad \forall x \in \partial D, \forall t \in [0, T]. \tag{8}$$

Throughout this chapter, we will assume $\boldsymbol{u} = 0$ on the boundary ∂D and is extended outside D by zero.

Additionally we can also write the evolution in weak form by multiplying Eq. 6 by a smooth test function $\tilde{\boldsymbol{u}}$ with $\tilde{\boldsymbol{u}} = 0$ on ∂D to get

$$(\ddot{\boldsymbol{u}}(t), \tilde{\boldsymbol{u}}) = (-\nabla PD^\epsilon(\boldsymbol{u}(t)), \tilde{\boldsymbol{u}}) + (b(t), \tilde{\boldsymbol{u}}).$$

We denote L^2 dot product of u, v as (u, v). An integration by parts easily shows for all smooth u, v taking zero boundary values that

$$(-\nabla PD^\epsilon(\boldsymbol{u}), \boldsymbol{v}) = -a^\epsilon(\boldsymbol{u}, \boldsymbol{v}),$$

where

$$\begin{aligned} a^\epsilon(\boldsymbol{u}, \boldsymbol{v}) \\ = \frac{2}{\epsilon^{d+1}\omega_d} \int_D \int_{H_\epsilon(x)} \omega(x)\omega(y) J^\epsilon(|y-x|) \\ f'(|y-x|S(\boldsymbol{u})^2)|y-x|S(\boldsymbol{u})S(\boldsymbol{v}) dy dx. \end{aligned} \tag{9}$$

Weak form of the evolution in terms of operator a^ϵ becomes

$$(\ddot{\boldsymbol{u}}(t), \tilde{\boldsymbol{u}}) + a^\epsilon(\boldsymbol{u}(t), \tilde{\boldsymbol{u}}) = (b(t), \tilde{\boldsymbol{u}}). \tag{10}$$

Last we introduce the peridynamic energy. The total energy $\mathcal{E}^\epsilon(\boldsymbol{u})(t)$ is given by the sum of kinetic and potential energy given by

$$\mathcal{E}^\epsilon(\boldsymbol{u})(t) = \frac{1}{2}||\dot{\boldsymbol{u}}(t)||_{L^2(D;\mathbb{R}^d)} + PD^\epsilon(\boldsymbol{u}(t)), \tag{11}$$

where potential energy PD^ϵ is given by

$$PD^\epsilon(\boldsymbol{u}) = \int_D \left[\frac{1}{\epsilon^d \omega_d} \int_{H_\epsilon(x)} W^\epsilon(S(\boldsymbol{u}), y-x) dy \right] dx.$$

We state the following equation which will be used later in the chapter

$$\frac{d}{dt}\mathcal{E}^\epsilon(\boldsymbol{u})(t) = (\ddot{\boldsymbol{u}}(t), \dot{\boldsymbol{u}}(t)) - (-\nabla PD^\epsilon(\boldsymbol{u}(t)), \dot{\boldsymbol{u}}(t)). \tag{12}$$

In order to develop the approximation theory in the following sections, we find it convenient to write the evolution Eq. 6 as an equivalent first order system with $y_1(t) = \boldsymbol{u}(t)$ and $y_2(t) = \boldsymbol{v}(t)$ with $\boldsymbol{v}(t) = \partial_t \boldsymbol{u}(t)$. Let $y = (y_1, y_2)^T$ where at each time y_1, y_2 belong to the same function space V, and let $F^\epsilon(y,t) = (F_1^\epsilon(y,t), F_2^\epsilon(y,t))^T$ such that

$$F_1^\epsilon(y,t) := y_2 \tag{13}$$

$$F_2^\epsilon(y,t) := -\nabla PD^\epsilon(y_1) + \boldsymbol{b}(t). \tag{14}$$

The initial boundary value associated with the evolution Eq. 6 is equivalent to the initial boundary value problem for the first order system given by

$$\frac{d}{dt}y = F^\epsilon(y,t), \tag{15}$$

with initial condition given by $y(0) = (\boldsymbol{u}_0, \boldsymbol{v}_0)^T \in X = V \times V$.

To establish the error estimates, we will use the Lipschitz property of the peridynamic force in $X = L^2(D;\mathbb{R}^d) \times L^2(D;\mathbb{R}^d)$. It is given by Theorem 6.1 of Lipton 2016.

Theorem 1.

$$||F^\epsilon(y,t) - F^\epsilon(z,t)||_X \leq \frac{L}{\epsilon^2}||y-z||_X \qquad \forall y,z \in X, \forall t \in [0,T] \tag{16}$$

for all $y, z \in L^2(D;\mathbb{R}^d)^2$.
Here L does not depend on $\boldsymbol{u}, \boldsymbol{v}$.

Finite Difference Approximation

In this section, we present the finite difference scheme and compute the rate of convergence. We also consider the semi-discrete approximation and prove the bound on energy of semi-discrete evolution in terms of initial energy and the work done by body forces.

Let h be the size of a mesh and Δt be the size of time step. We will keep ϵ fixed and assume that $h < \epsilon < 1$. Let $D_h = D \cap (h\mathbb{Z})^d$ be the discretization of material domain. Let $i \in \mathbb{Z}^d$ be the index such that $\boldsymbol{x}_i = hi \in D$. Let U_i be the unit cell of volume h^d corresponding to the grid point $\boldsymbol{x}_i$, see Fig. 3. The exact solution evaluated at grid points is denoted by $(\boldsymbol{u}_i(t), \boldsymbol{v}_i(t))$.

Time Discretization

Let $[0,T] \cap (\Delta t\mathbb{Z})$ be the discretization of time domain where Δt is the size of time step. Denote fully discrete solution at $(t^k = k\Delta t, \boldsymbol{x}_i = ih)$ as $(\hat{\boldsymbol{u}}_i^k, \hat{\boldsymbol{v}}_i^k)$. Similarly, the exact solution evaluated at space-time grid points is denoted by $(\boldsymbol{u}_i^k, \boldsymbol{v}_i^k)$. We enforce the boundary condition $\hat{\boldsymbol{u}}_i^k = \boldsymbol{0}$ for all $\boldsymbol{x}_i \notin D$ and for all k.

We begin with the forward Euler time discretization, with respect to velocity, and the finite difference scheme for $(\hat{\boldsymbol{u}}_i^k, \hat{\boldsymbol{v}}_i^k)$ is written

$$\frac{\hat{\boldsymbol{u}}_i^{k+1} - \hat{\boldsymbol{u}}_i^k}{\Delta t} = \hat{\boldsymbol{v}}_i^{k+1} \tag{17}$$

$$\frac{\hat{\boldsymbol{v}}_i^{k+1} - \hat{\boldsymbol{v}}_i^k}{\Delta t} = -\nabla PD^\epsilon(\hat{\boldsymbol{u}}^k)(\boldsymbol{x}_i) + \boldsymbol{b}_i^k \tag{18}$$

The scheme is complemented with the discretized initial conditions $\hat{\boldsymbol{u}}_i^0 = (\hat{\boldsymbol{u}}_0)_i$ and $\hat{\boldsymbol{v}}_i^0 = (\hat{\boldsymbol{v}}_0)_i$. If we substitute Eq. 17 into Eq. 18, we get the standard central difference scheme in time for second order in time differential equation. Here we have assumed, without loss of generality, $\rho = 1$.

The piecewise constant extensions of the discrete sets $\{\hat{\boldsymbol{u}}_i^k\}_{i \in \mathbb{Z}^d}$ and $\{\hat{\boldsymbol{v}}_i^k\}_{i \in \mathbb{Z}^d}$ are given by

$$\hat{\boldsymbol{u}}^k(\boldsymbol{x}) := \sum_{i, \boldsymbol{x}_i \in D} \hat{\boldsymbol{u}}_i^k \chi_{U_i}(\boldsymbol{x})$$

$$\hat{\boldsymbol{v}}^k(\boldsymbol{x}) := \sum_{i, \boldsymbol{x}_i \in D} \hat{\boldsymbol{v}}_i^k \chi_{U_i}(\boldsymbol{x})$$

In this way we represent the finite difference solution as a piecewise constant function. We will show that this function provides an L^2 approximation of the exact solution.

Convergence Results

In this section we provide upper bounds on the rate of convergence of the discrete approximation to the solution of the peridynamic evolution. The L^2 approximation error E^k at time t^k, for $0 < t^k \leq T$, is defined as

$$E^k := \left\| \hat{\boldsymbol{u}}^k - \boldsymbol{u}^k \right\|_{L^2(D;\mathbb{R}^d)} + \left\| \hat{\boldsymbol{v}}^k - \boldsymbol{v}^k \right\|_{L^2(D;\mathbb{R}^d)}$$

The upper bound on the convergence rate of the approximation error is given by the following theorem.

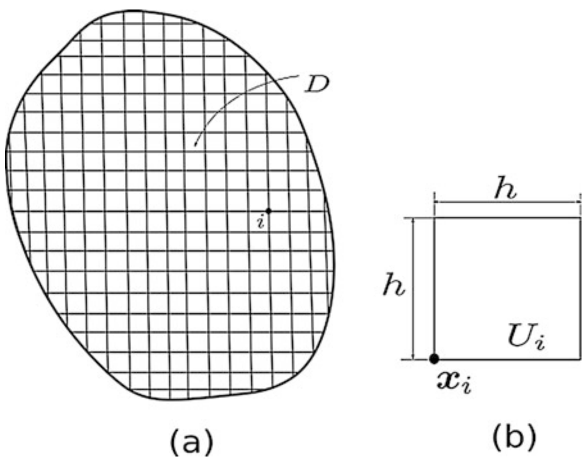

Fig. 3 (**a**) Typical mesh of size h. (**b**) Unit cell U_i corresponding to material point $\boldsymbol{x}_i$

Theorem 2 (Convergence of finite difference approximation (forward Euler time discretization)). *Let $\epsilon > 0$ be fixed. Let $(\boldsymbol{u}, \boldsymbol{v})$ be the solution of peridynamic equation Eq. 15. We assume $\boldsymbol{u}, \boldsymbol{v} \in C^2([0,T]; C_0^{0,\gamma}(D;\mathbb{R}^d))$. Then the forward Euler time discretization, and finite difference spatial discretization scheme given by Eqs. 17 and 18, is consistent in both time and spatial discretization and converges to the exact solution uniformly in time with respect to the $L^2(D;\mathbb{R}^d)$ norm. If we assume the error at the initial step is zero, then the error E^k at time t^k is bounded and to leading order in the time step Δt satisfies*

$$\sup_{0 \le k \le T/\Delta t} E^k \le O\left(C_t \Delta t + C_s \frac{h^\gamma}{\epsilon^2}\right), \tag{19}$$

where constants C_s and C_t are independent of h and Δt and C_s depends on the Hölder norm of the solution and C_t depends on the L^2 norms of time derivatives of the solution.

Here we have assumed the initial error to be zero for ease of exposition only.

We remark that the explicit constants leading to Eq. 19 can be large. The inequality that delivers Eq. 19 is given to leading order by

$$\sup_{0 \le k \le T/\Delta t} E^k \le \exp\left[T(1 + 6\bar{C}/\epsilon^2)\right] T \left[C_t \Delta t + (C_s/\epsilon^2) h^\gamma\right], \tag{20}$$

where the constants $\bar{C}$, C_t, and C_s are given by Eqs. 43, 45, and 46. The explicit constant C_t depends on the spatial L^2 norm of the time derivatives of the solution, and C_s depends on the spatial Hölder continuity of the solution and the constant $\bar{C}$. This constant is bounded independently of horizon ϵ. Although the constants are necessarily pessimistic, they deliver a priori error estimates. These constants are discussed in Jha and Lipton (2017a) in the context of fracture experiments. Fracture experiments are on the order of hundreds of μ-sec, and the size of the constants in the estimate for finite element simulations remains small for tens of μ-sec. For finite element schemes, we have a priori estimates with constants that stay small for same order of magnitude in time as fracture experiments. These features are discussed in Jha and Lipton (2017a,b).

Error Analysis

We define the L^2 projections of the actual solutions onto the space of piecewise constant functions defined over the cells U_i. These are given as follows. Let $(\tilde{\boldsymbol{u}}_i^k, \tilde{\boldsymbol{v}}_i^k)$ be the average of the exact solution $(\boldsymbol{u}^k, \boldsymbol{v}^k)$ in the unit cell U_i given by

$$\tilde{\boldsymbol{u}}_i^k := \frac{1}{h^d} \int_{U_i} \boldsymbol{u}^k(\boldsymbol{x}) d\boldsymbol{x}$$

$$\tilde{\boldsymbol{v}}_i^k := \frac{1}{h^d} \int_{U_i} \boldsymbol{v}^k(\boldsymbol{x}) d\boldsymbol{x}$$

and the L^2 projection of the solution onto piecewise constant functions is $(\tilde{\boldsymbol{u}}^k, \tilde{\boldsymbol{v}}^k)$ given by

$$\tilde{\boldsymbol{u}}^k(\boldsymbol{x}) := \sum_{i, \boldsymbol{x}_i \in D} \tilde{\boldsymbol{u}}_i^k \chi_{U_i}(\boldsymbol{x}) \tag{21}$$

$$\tilde{\boldsymbol{v}}^k(\boldsymbol{x}) := \sum_{i, \boldsymbol{x}_i \in D} \tilde{\boldsymbol{v}}_i^k \chi_{U_i}(\boldsymbol{x}) \tag{22}$$

The error between $(\hat{\boldsymbol{u}}^k, \hat{\boldsymbol{v}}^k)^T$ and $(\boldsymbol{u}(t^k), \boldsymbol{v}(t^k))^T$ is now split into two parts. From the triangle inequality, we have

$$\left\|\hat{\boldsymbol{u}}^k - \boldsymbol{u}(t^k)\right\|_{L^2(D;\mathbb{R}^d)} \leq \left\|\hat{\boldsymbol{u}}^k - \tilde{\boldsymbol{u}}^k\right\|_{L^2(D;\mathbb{R}^d)} + \left\|\tilde{\boldsymbol{u}}^k - \boldsymbol{u}^k\right\|_{L^2(D;\mathbb{R}^d)}$$
$$\left\|\hat{\boldsymbol{v}}^k - \boldsymbol{v}(t^k)\right\|_{L^2(D;\mathbb{R}^d)} \leq \left\|\hat{\boldsymbol{v}}^k - \tilde{\boldsymbol{v}}^k\right\|_{L^2(D;\mathbb{R}^d)} + \left\|\tilde{\boldsymbol{v}}^k - \boldsymbol{v}^k\right\|_{L^2(D;\mathbb{R}^d)}$$

In section "Error Analysis for Approximation of L^2 Projection of the Exact Solution" we will show that the error between the L^2 projections of the actual solution and the discrete approximation decays according to

$$\sup_{0 \leq k \leq T/\Delta t} \left(\left\|\hat{\boldsymbol{u}}^k - \tilde{\boldsymbol{u}}^k\right\|_{L^2(D;\mathbb{R}^d)} + \left\|\hat{\boldsymbol{v}}^k - \tilde{\boldsymbol{v}}^k\right\|_{L^2(D;\mathbb{R}^d)} \right) = O\left(\Delta t + \frac{h^\gamma}{\epsilon^2}\right). \tag{23}$$

In what follows we can estimate the terms

$$\left\|\tilde{\boldsymbol{u}}^k - \boldsymbol{u}(t^k)\right\|_{L^2()} \text{ and } \left\|\tilde{\boldsymbol{v}}^k - \boldsymbol{v}(t^k)\right\|_{L^2()} \tag{24}$$

and show they go to zero at a rate of h^γ uniformly in time. The estimates given by Eq. 23 together with the $O(h^\gamma)$ estimates for Eq. 24 establish Theorem 2. We now establish the L^2 estimates for the differences $\tilde{\boldsymbol{u}}^k - \boldsymbol{u}(t^k)$ and $\tilde{\boldsymbol{v}}^k - \boldsymbol{v}(t^k)$.

We write

$$\begin{aligned}
&\left\|\tilde{\boldsymbol{u}}^k - \boldsymbol{u}^k\right\|^2_{L^2(D;\mathbb{R}^d)} \\
&= \sum_{i, \boldsymbol{x}_i \in D} \int_{U_i} \left|\tilde{\boldsymbol{u}}^k(\boldsymbol{x}) - \boldsymbol{u}^k(\boldsymbol{x})\right|^2 d\boldsymbol{x} \\
&= \sum_{i, \boldsymbol{x}_i \in D} \int_{U_i} \left|\frac{1}{h^d} \int_{U_i} (\boldsymbol{u}^k(\boldsymbol{y}) - \boldsymbol{u}^k(\boldsymbol{x})) d\boldsymbol{y}\right|^2 d\boldsymbol{x} \\
&= \sum_{i, \boldsymbol{x}_i \in D} \int_{U_i} \left[\frac{1}{h^{2d}} \int_{U_i} \int_{U_i} (\boldsymbol{u}^k(\boldsymbol{y}) - \boldsymbol{u}^k(\boldsymbol{x})) \cdot (\boldsymbol{u}^k(\boldsymbol{z}) - \boldsymbol{u}^k(\boldsymbol{x})) d\boldsymbol{y} d\boldsymbol{z}\right] d\boldsymbol{x}
\end{aligned}$$

$$\leq \sum_{i, \boldsymbol{x}_i \in D} \int_{U_i} \left[\frac{1}{h^d} \int_{U_i} \left| \boldsymbol{u}^k(\boldsymbol{y}) - \boldsymbol{u}^k(\boldsymbol{x}) \right|^2 d\boldsymbol{y} \right] d\boldsymbol{x} \tag{25}$$

where we used Cauchy's inequality and Jensen's inequality. For $\boldsymbol{x}, \boldsymbol{y} \in U_i$, $|\boldsymbol{x} - \boldsymbol{y}| \leq ch$, where $c = \sqrt{2}$ for $d = 2$ and $c = \sqrt{3}$ for $d = 3$. Since $\boldsymbol{u} \in C_0^{0,\gamma}$ we have

$$\begin{aligned} \left| \boldsymbol{u}^k(\boldsymbol{x}) - \boldsymbol{u}^k(\boldsymbol{y}) \right| &= |\boldsymbol{x} - \boldsymbol{y}|^\gamma \frac{\left| \boldsymbol{u}^k(\boldsymbol{y}) - \boldsymbol{u}^k(\boldsymbol{x}) \right|}{|\boldsymbol{x} - \boldsymbol{y}|^\gamma} \\ &\leq c^\gamma h^\gamma \left\| \boldsymbol{u}^k \right\|_{C^{0,\gamma}(D;\mathbb{R}^d)} \leq c^\gamma h^\gamma \sup_t \|\boldsymbol{u}(t)\|_{C^{0,\gamma}(D;\mathbb{R}^d)} \end{aligned} \tag{26}$$

and substitution in Eq. 25 gives

$$\begin{aligned} \left\| \tilde{\boldsymbol{u}}^k - \boldsymbol{u}^k \right\|^2_{L^2(D;\mathbb{R}^d)} &\leq c^{2\gamma} h^{2\gamma} \sum_{i, \boldsymbol{x}_i \in D} \int_{U_i} d\boldsymbol{x} \left(\sup_t \|\boldsymbol{u}(t)\|_{C^{0,\gamma}(D;\mathbb{R}^d)} \right)^2 \\ &\leq c^{2\gamma} |D| h^{2\gamma} \left(\sup_t \|\boldsymbol{u}(t)\|_{C^{0,\gamma}(D;\mathbb{R}^d)} \right)^2 . \end{aligned}$$

A similar estimate can be derived for $||\tilde{\boldsymbol{v}}^k - \boldsymbol{v}^k||_{L^2}$, and substitution of the estimates into Eq. 24 gives

$$\sup_k \left(\left\| \tilde{\boldsymbol{u}}^k - \boldsymbol{u}(t^k) \right\|_{L^2(D;\mathbb{R}^d)} + \left\| \tilde{\boldsymbol{v}}^k - \boldsymbol{v}(t^k) \right\|_{L^2(D;\mathbb{R}^d)} \right) = O(h^\gamma).$$

In the next section, we establish the error estimate (Eq. 23) for forward Euler in section "Error Analysis for Approximation of L^2 Projection of the Exact Solution".

Error Analysis for Approximation of L^2 Projection of the Exact Solution

In this subsection, we estimate the difference between approximate solution $(\hat{\boldsymbol{u}}^k, \hat{\boldsymbol{v}}^k)$ and the L^2 projection of the exact solution onto piecewise constant functions given by $(\tilde{\boldsymbol{u}}^k, \tilde{\boldsymbol{v}}^k)$ (see Eqs. 21 and 22). Let the differences be denoted by $\boldsymbol{e}^k(u) := \hat{\boldsymbol{u}}^k - \tilde{\boldsymbol{u}}^k$ and $\boldsymbol{e}^k(v) := \hat{\boldsymbol{v}}^k - \tilde{\boldsymbol{v}}^k$, and their evaluations at grid points are $\boldsymbol{e}_i^k(u) := \hat{\boldsymbol{u}}_i^k - \tilde{\boldsymbol{u}}_i^k$ and $\boldsymbol{e}_i^k(v) := \hat{\boldsymbol{v}}_i^k - \tilde{\boldsymbol{v}}_i^k$. Subtracting $(\tilde{\boldsymbol{u}}_i^{k+1} - \tilde{\boldsymbol{u}}_i^k)/\Delta t$ from Eq. 17 gives

$$\begin{aligned} &\frac{\hat{\boldsymbol{u}}_i^{k+1} - \hat{\boldsymbol{u}}_i^k}{\Delta t} - \frac{\tilde{\boldsymbol{u}}_i^{k+1} - \tilde{\boldsymbol{u}}_i^k}{\Delta t} \\ &= \hat{\boldsymbol{v}}_i^{k+1} - \frac{\tilde{\boldsymbol{u}}_i^{k+1} - \tilde{\boldsymbol{u}}_i^k}{\Delta t} \\ &= \hat{\boldsymbol{v}}_i^{k+1} - \tilde{\boldsymbol{v}}_i^{k+1} + \left(\tilde{\boldsymbol{v}}_i^{k+1} - \frac{\partial \tilde{\boldsymbol{u}}_i^{k+1}}{\partial t} \right) + \left(\frac{\partial \tilde{\boldsymbol{u}}_i^{k+1}}{\partial t} - \frac{\tilde{\boldsymbol{u}}_i^{k+1} - \tilde{\boldsymbol{u}}_i^k}{\Delta t} \right). \end{aligned}$$

Taking the average over unit cell U_i of the exact peridynamic equation Eq. 15 at time t^k, we will get $\tilde{\boldsymbol{v}}_i^{k+1} - \frac{\partial \tilde{\boldsymbol{u}}_i^{k+1}}{\partial t} = 0$. Therefore, the equation for $\boldsymbol{e}_i^k(u)$ is given by

$$\boldsymbol{e}_i^{k+1}(u) = \boldsymbol{e}_i^k(u) + \Delta t \boldsymbol{e}_i^{k+1}(v) + \Delta t \tau_i^k(u), \tag{27}$$

where we identify the discretization error as

$$\tau_i^k(u) := \frac{\partial \tilde{\boldsymbol{u}}_i^{k+1}}{\partial t} - \frac{\tilde{\boldsymbol{u}}_i^{k+1} - \tilde{\boldsymbol{u}}_i^k}{\Delta t}. \tag{28}$$

Similarly, we subtract $(\tilde{\boldsymbol{v}}_i^{k+1} - \tilde{\boldsymbol{v}}_i^k)/\Delta t$ from Eq. 18 and add and subtract terms to get

$$\begin{aligned}
\frac{\hat{\boldsymbol{v}}_i^{k+1} - \hat{\boldsymbol{v}}_i^k}{\Delta t} - \frac{\tilde{\boldsymbol{v}}_i^{k+1} - \tilde{\boldsymbol{v}}_i^k}{\Delta t} &= -\boldsymbol{\nabla} PD^\epsilon(\hat{\boldsymbol{u}}^k)(\boldsymbol{x}_i) + \boldsymbol{b}_i^k - \frac{\partial \boldsymbol{v}_i^k}{\partial t} + \left(\frac{\partial \boldsymbol{v}_i^k}{\partial t} - \frac{\tilde{\boldsymbol{v}}_i^{k+1} - \tilde{\boldsymbol{v}}_i^k}{\Delta t} \right) \\
&= -\boldsymbol{\nabla} PD^\epsilon(\hat{\boldsymbol{u}}^k)(\boldsymbol{x}_i) + \boldsymbol{b}_i^k - \frac{\partial \boldsymbol{v}_i^k}{\partial t} \\
&\quad + \left(\frac{\partial \tilde{\boldsymbol{v}}_i^k}{\partial t} - \frac{\tilde{\boldsymbol{v}}_i^{k+1} - \tilde{\boldsymbol{v}}_i^k}{\Delta t} \right) + \left(\frac{\partial \boldsymbol{v}_i^k}{\partial t} - \frac{\partial \tilde{\boldsymbol{v}}_i^k}{\partial t} \right),
\end{aligned} \tag{29}$$

where we identify $\tau_i^k(v)$ as follows

$$\tau_i^k(v) := \frac{\partial \tilde{\boldsymbol{v}}_i^k}{\partial t} - \frac{\tilde{\boldsymbol{v}}_i^{k+1} - \tilde{\boldsymbol{v}}_i^k}{\Delta t}. \tag{30}$$

Note that in $\tau^k(u)$ we have $\frac{\partial \tilde{\boldsymbol{u}}_i^{k+1}}{\partial t}$, and from the exact peridynamic equation, we have

$$\boldsymbol{b}_i^k - \frac{\partial \boldsymbol{v}_i^k}{\partial t} = \nabla PD^\epsilon(\boldsymbol{u}^k)(\boldsymbol{x}_i). \tag{31}$$

Combining Eqs. 29, 30, and 31 gives

$$\begin{aligned}
\boldsymbol{e}_i^{k+1}(v) = \boldsymbol{e}_i^k(v) + \Delta t \tau_i^k(v) + \Delta t \left(\frac{\partial \boldsymbol{v}_i^k}{\partial t} - \frac{\partial \tilde{\boldsymbol{v}}_i^k}{\partial t} \right) \\
+ \Delta t \left(-\boldsymbol{\nabla} PD^\epsilon(\hat{\boldsymbol{u}}^k)(\boldsymbol{x}_i) + \boldsymbol{\nabla} PD^\epsilon(\boldsymbol{u}^k)(\boldsymbol{x}_i) \right)
\end{aligned}$$

$$= \boldsymbol{e}_i^k(v) + \Delta t \tau_i^k(v) + \Delta t \left(\frac{\partial \boldsymbol{v}_i^k}{\partial t} - \frac{\partial \tilde{\boldsymbol{v}}_i^k}{\partial t} \right)$$

$$+ \Delta t \left(-\nabla PD^\epsilon(\hat{\boldsymbol{u}}^k)(\boldsymbol{x}_i) + \nabla PD^\epsilon(\tilde{\boldsymbol{u}}^k)(\boldsymbol{x}_i) \right)$$

$$+ \Delta t \left(-\nabla PD^\epsilon(\tilde{\boldsymbol{u}}^k)(\boldsymbol{x}_i) + \nabla PD^\epsilon(\boldsymbol{u}^k)(\boldsymbol{x}_i) \right).$$

The spatial discretization error $\sigma_i^k(u)$ and $\sigma_i^k(v)$ is given by

$$\sigma_i^k(u) := \left(-\nabla PD^\epsilon(\tilde{\boldsymbol{u}}^k)(\boldsymbol{x}_i) + \nabla PD^\epsilon(\boldsymbol{u}^k)(\boldsymbol{x}_i) \right) \tag{32}$$

$$\sigma_i^k(v) := \frac{\partial \boldsymbol{v}_i^k}{\partial t} - \frac{\partial \tilde{\boldsymbol{v}}_i^k}{\partial t}. \tag{33}$$

We finally have

$$\boldsymbol{e}_i^{k+1}(v) = \boldsymbol{e}_i^k(v) + \Delta t \left(\tau_i^k(v) + \sigma_i^k(u) + \sigma_i^k(v) \right)$$
$$+ \Delta t \left(-\nabla PD^\epsilon(\hat{\boldsymbol{u}}^k)(\boldsymbol{x}_i) + \nabla PD^\epsilon(\tilde{\boldsymbol{u}}^k)(\boldsymbol{x}_i) \right). \tag{34}$$

We now show the consistency and stability properties of the numerical scheme.

Consistency

We deal with the error in time discretization and the error in spatial discretization error separately. The time discretization error follows easily using the Taylor's series, while the spatial discretization error uses properties of the nonlinear peridynamic force.

Time discretization: We first estimate the time discretization error. A Taylor series expansion is used to estimate $\tau_i^k(u)$ as follows

$$\tau_i^k(u) = \frac{1}{h^d} \int_{U_i} \left(\frac{\partial \boldsymbol{u}^k(\boldsymbol{x})}{\partial t} - \frac{\boldsymbol{u}^{k+1}(\boldsymbol{x}) - \boldsymbol{u}^k(\boldsymbol{x})}{\Delta t} \right) d\boldsymbol{x}$$
$$= \frac{1}{h^d} \int_{U_i} \left(-\frac{1}{2} \frac{\partial^2 \boldsymbol{u}^k(\boldsymbol{x})}{\partial t^2} \Delta t + O((\Delta t)^2) \right) d\boldsymbol{x}.$$

Computing the L^2 norm of $\tau_i^k(u)$ and using Jensen's inequality gives

$$\left\| \tau^k(u) \right\|_{L^2(D;\mathbb{R}^d)} \leq \frac{\Delta t}{2} \left\| \frac{\partial^2 \boldsymbol{u}^k}{\partial t^2} \right\|_{L^2(D;\mathbb{R}^d)} + O((\Delta t)^2)$$
$$\leq \frac{\Delta t}{2} \sup_t \left\| \frac{\partial^2 \boldsymbol{u}(t)}{\partial t^2} \right\|_{L^2(D;\mathbb{R}^d)} + O((\Delta t)^2).$$

Similarly, we have

$$\left\| \tau^k(v) \right\|_{L^2(D;\mathbb{R}^d)} = \frac{\Delta t}{2} \sup_t \left\| \frac{\partial^2 \boldsymbol{v}(t)}{\partial t^2} \right\|_{L^2(D;\mathbb{R}^d)} + O((\Delta t)^2).$$

Spatial discretization: We now estimate the spatial discretization error. Substituting the definition of $\tilde{\boldsymbol{v}}^k$ and following the similar steps employed in Eq. 26 gives

$$\left|\sigma_i^k(v)\right| = \left| \frac{\partial \boldsymbol{v}_i^k}{\partial t} - \frac{1}{h^d} \int_{U_i} \frac{\partial \boldsymbol{v}^k(\boldsymbol{x})}{\partial t} d\boldsymbol{x} \right| \leq c^\gamma h^\gamma \int_{U_i} \frac{1}{|\boldsymbol{x}_i - \boldsymbol{x}|^\gamma} \left| \frac{\partial \boldsymbol{v}^k(\boldsymbol{x}_i)}{\partial t} - \frac{\partial \boldsymbol{v}^k(\boldsymbol{x})}{\partial t} \right| d\boldsymbol{x}$$
$$\leq c^\gamma h^\gamma \left\| \frac{\partial \boldsymbol{v}^k}{\partial t} \right\|_{C^{0,\gamma}(D;\mathbb{R}^d)} \leq c^\gamma h^\gamma \sup_t \left\| \frac{\partial \boldsymbol{v}(t)}{\partial t} \right\|_{C^{0,\gamma}(D;\mathbb{R}^d)}.$$

Taking the L^2 norm of error $\sigma_i^k(v)$ and substituting the estimate above delivers

$$\left\| \sigma^k(v) \right\|_{L^2(D;\mathbb{R}^d)} \leq h^\gamma c^\gamma \sqrt{|D|} \sup_t \left\| \frac{\partial \boldsymbol{v}(t)}{\partial t} \right\|_{C^{0,\gamma}(D;\mathbb{R}^d)}.$$

Now we estimate $\left|\sigma_i^k(u)\right|$. Note that the force $-\nabla PD^\epsilon(\boldsymbol{u})(\boldsymbol{x})$ can be written as follows

$$-\nabla PD^\epsilon(\boldsymbol{u})(\boldsymbol{x}) = \frac{4}{\epsilon^{d+1}\omega_d} \int_{H_\epsilon(\boldsymbol{x})} \omega(\boldsymbol{x})\omega(\boldsymbol{y}) J\left(\frac{|\boldsymbol{y}-\boldsymbol{x}|}{\epsilon}\right) f'(|\boldsymbol{y}-\boldsymbol{x}|\, S(\boldsymbol{y},\boldsymbol{x};\boldsymbol{u})^2)$$
$$S(\boldsymbol{y},\boldsymbol{x};\boldsymbol{u}) \frac{\boldsymbol{y}-\boldsymbol{x}}{|\boldsymbol{y}-\boldsymbol{x}|} d\boldsymbol{y} = \frac{4}{\epsilon\omega_d} \int_{H_1(\boldsymbol{0})} \omega(\boldsymbol{x})\omega(\boldsymbol{x}+\epsilon\boldsymbol{\xi}) J(|\boldsymbol{\xi}|) f'(\epsilon\, |\boldsymbol{\xi}|$$
$$S(\boldsymbol{x}+\epsilon\boldsymbol{\xi},\boldsymbol{x};\boldsymbol{u})^2) S(\boldsymbol{x}+\epsilon\boldsymbol{\xi},\boldsymbol{x};\boldsymbol{u}) \frac{\boldsymbol{\xi}}{|\boldsymbol{\xi}|} d\boldsymbol{\xi}.$$

where we substituted $\partial_S W^\epsilon$ using Eq. 2. In the second step, we introduced the change in variable $\boldsymbol{y} = \boldsymbol{x} + \epsilon\boldsymbol{\xi}$.

Let $F_1 : \mathbb{R} \to \mathbb{R}$ be defined as $F_1(S) = f(S^2)$. Then $F_1'(S) = f'(S^2)2S$. Using the definition of F_1, we have

$$2Sf'(\epsilon\, |\boldsymbol{\xi}|\, S^2) = \frac{F_1'(\sqrt{\epsilon\, |\boldsymbol{\xi}|} S)}{\sqrt{\epsilon\, |\boldsymbol{\xi}|}}.$$

Because f is assumed to be positive, smooth, and concave and is bounded far away, we have the following bound on derivatives of F_1

$$\sup_r \left| F_1'(r) \right| = F_1'(\bar{r}) =: C_1 \tag{35}$$

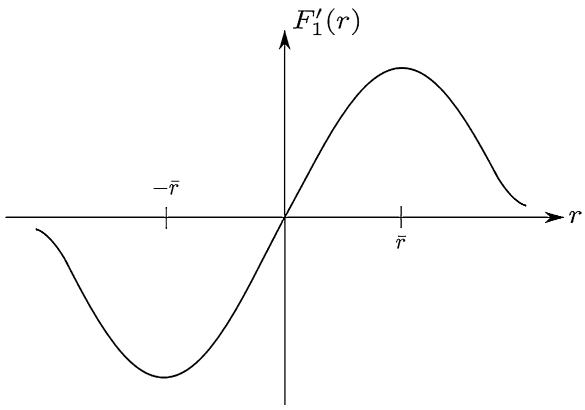

Fig. 4 Generic plot of $F_1'(r)$. $|F_1'(r)|$ is bounded by $\left|F_1'(\bar{r})\right|$

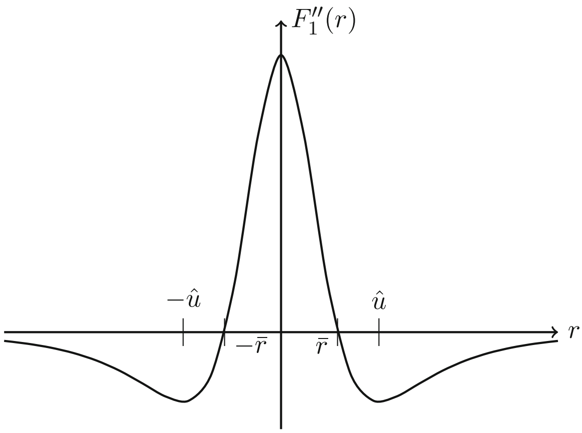

Fig. 5 Generic plot of $F_1''(r)$. At $\pm\bar{r}$, $F_1''(r) = 0$. At $\pm\hat{u}$, $F_1'''(r) = 0$

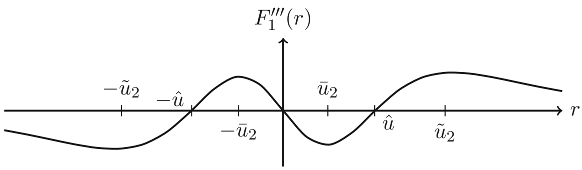

Fig. 6 Generic plot of $F_1'''(r)$. At $\pm\bar{u}_2$ and $\pm\tilde{u}_2$, $F_1'''' = 0$

$$\sup_r \left|F_1''(r)\right| = \max\{F_1''(0), F_1''(\hat{u})\} =: C_2 \tag{36}$$

$$\sup_r \left|F_1'''(r)\right| = \max\{F_1'''(\bar{u}_2), F_1'''(\tilde{u}_2)\} =: C_3. \tag{37}$$

where $\bar{r}$ is the inflection point of $f(r^2)$, i.e., $F_1''(\bar{r}) = 0$. $\{0, \hat{u}\}$ are the maxima of $F_1''(r)$. $\{\bar{u}, \tilde{u}\}$ are the maxima of $F_1'''(r)$. By chain rule and by considering the assumption on f, we can show that $\bar{r}, \hat{u}, \bar{u}_2, \tilde{u}_2$ exist and the C_1, C_2, C_3 are bounded. Figures 4, 5, and 6 show the generic graphs of $F_1'(r)$, $F_1''(r)$, and $F_1'''(r)$, respectively.

The nonlocal force $-\nabla PD^\epsilon$ can be written as

$$
\begin{aligned}
&-\nabla PD^\epsilon(\boldsymbol{u})(\boldsymbol{x})\\
&= \frac{2}{\epsilon\omega_d}\int_{H_1(\mathbf{0})} \omega(\boldsymbol{x})\omega(\boldsymbol{x}+\epsilon\boldsymbol{\xi})J(|\boldsymbol{\xi}|)F_1'(\sqrt{\epsilon\,|\boldsymbol{\xi}|}S(\boldsymbol{x}+\epsilon\boldsymbol{\xi},\boldsymbol{x};\boldsymbol{u}))\frac{1}{\sqrt{\epsilon\,|\boldsymbol{\xi}|}}\frac{\boldsymbol{\xi}}{|\boldsymbol{\xi}|}d\boldsymbol{\xi}.
\end{aligned}
\tag{38}
$$

To simplify the calculations, we use the following notation

$$
\begin{aligned}
\bar{\boldsymbol{u}}(\boldsymbol{x}) &:= \boldsymbol{u}(\boldsymbol{x}+\epsilon\boldsymbol{\xi})-\boldsymbol{u}(\boldsymbol{x}),\\
\bar{\boldsymbol{u}}(\boldsymbol{y}) &:= \boldsymbol{u}(\boldsymbol{y}+\epsilon\boldsymbol{\xi})-\boldsymbol{u}(\boldsymbol{y}),\\
(\boldsymbol{u}-\boldsymbol{v})(\boldsymbol{x}) &:= \boldsymbol{u}(\boldsymbol{x})-\boldsymbol{v}(\boldsymbol{x}),
\end{aligned}
$$

and $\overline{(\boldsymbol{u}-\boldsymbol{v})}(\boldsymbol{x})$ is defined similar to $\bar{\boldsymbol{u}}(\boldsymbol{x})$. Also, let

$$
s=\epsilon\,|\boldsymbol{\xi}|\,,\quad \boldsymbol{e}=\frac{\boldsymbol{\xi}}{|\boldsymbol{\xi}|}.
$$

In what follows, we will come across the integral of type $\int_{H_1(\mathbf{0})} J(|\boldsymbol{\xi}|)\,|\boldsymbol{\xi}|^{-\alpha}\,d\boldsymbol{\xi}$. Recall that $0\le J(|\boldsymbol{\xi}|)\le M$ for all $\boldsymbol{\xi}\in H_1(\mathbf{0})$ and $J(|\boldsymbol{\xi}|)=0$ for $\boldsymbol{\xi}\notin H_1(\mathbf{0})$. Therefore, let

$$
\bar{J}_\alpha := \frac{1}{\omega_d}\int_{H_1(\mathbf{0})} J(|\boldsymbol{\xi}|)\,|\boldsymbol{\xi}|^{-\alpha}\,d\boldsymbol{\xi}.
\tag{39}
$$

With notations above, we note that $S(\boldsymbol{x}+\epsilon\boldsymbol{\xi},\boldsymbol{x};\boldsymbol{u})=\bar{\boldsymbol{u}}(\boldsymbol{x})\cdot\boldsymbol{e}/s$. $-\nabla PD^\epsilon$ can be written as

$$
-\nabla PD^\epsilon(\boldsymbol{u})(\boldsymbol{x}) = \frac{2}{\epsilon\omega_d}\int_{H_1(\mathbf{0})} \omega(\boldsymbol{x})\omega(\boldsymbol{x}+\epsilon\boldsymbol{\xi})J(|\boldsymbol{\xi}|)F_1'(\bar{\boldsymbol{u}}(\boldsymbol{x})\cdot\boldsymbol{e}/\sqrt{s})\frac{1}{\sqrt{s}}\boldsymbol{e}\,d\boldsymbol{\xi}.
\tag{40}
$$

We estimate $|-\nabla PD^\epsilon(\boldsymbol{u})(\boldsymbol{x})-(-\nabla PD^\epsilon(\boldsymbol{v})(\boldsymbol{x}))|$.

$$
\begin{aligned}
&|-\nabla PD^\epsilon(\boldsymbol{u})(\boldsymbol{x})-(-\nabla PD^\epsilon(\boldsymbol{v})(\boldsymbol{x}))|\\
&\le \left|\frac{2}{\epsilon\omega_d}\int_{H_1(\mathbf{0})} \omega(\boldsymbol{x})\omega(\boldsymbol{x}+\epsilon\boldsymbol{\xi})J(|\boldsymbol{\xi}|)\frac{\left(F_1'(\bar{\boldsymbol{u}}(\boldsymbol{x})\cdot\boldsymbol{e}/\sqrt{s})-F_1'(\bar{\boldsymbol{v}}(\boldsymbol{x})\cdot\boldsymbol{e}/\sqrt{s})\right)}{\sqrt{s}}\boldsymbol{e}\,d\boldsymbol{\xi}\right|\\
&\le \left|\frac{2}{\epsilon\omega_d}\int_{H_1(\mathbf{0})} J(|\boldsymbol{\xi}|)\frac{1}{\sqrt{s}}\left|F_1'(\bar{\boldsymbol{u}}(\boldsymbol{x})\cdot\boldsymbol{e}/\sqrt{s})-F_1'(\bar{\boldsymbol{v}}(\boldsymbol{x})\cdot\boldsymbol{e}/\sqrt{s})\right|d\boldsymbol{\xi}\right|\\
&\le \sup_r\left|F_1''(r)\right|\left|\frac{2}{\epsilon\omega_d}\int_{H_1(\mathbf{0})} J(|\boldsymbol{\xi}|)\frac{1}{\sqrt{s}}\left|\bar{\boldsymbol{u}}(\boldsymbol{x})\cdot\boldsymbol{e}/\sqrt{s}-\bar{\boldsymbol{v}}(\boldsymbol{x})\cdot\boldsymbol{e}/\sqrt{s}\right|d\boldsymbol{\xi}\right|
\end{aligned}
$$

$$\leq \frac{2C_2}{\epsilon\omega_d}\left|\int_{H_1(\mathbf{0})} J(|\boldsymbol{\xi}|)\frac{|\bar{\boldsymbol{u}}(\boldsymbol{x})-\bar{\boldsymbol{v}}(\boldsymbol{x})|}{\epsilon\,|\boldsymbol{\xi}|}d\boldsymbol{\xi}\right|. \tag{41}$$

Here we have used the fact that $|\omega(\boldsymbol{x})| \leq 1$ and for a vector $\boldsymbol{e}$ such that $|\boldsymbol{e}| = 1$, $|\mathbf{a}\cdot\boldsymbol{e}| \leq |\mathbf{a}|$ holds and $|\alpha\boldsymbol{e}| \leq |\alpha|$ holds for all $\mathbf{a} \in \mathbb{R}^d, \alpha \in \mathbb{R}$.

We use the notation $\bar{\boldsymbol{u}}^k(\boldsymbol{x}) := \boldsymbol{u}^k(\boldsymbol{x}+\epsilon\boldsymbol{\xi}) - \boldsymbol{u}^k(\boldsymbol{x})$ and $\bar{\tilde{\boldsymbol{u}}}^k(\boldsymbol{x}) := \tilde{\boldsymbol{u}}(\boldsymbol{x}+\epsilon\boldsymbol{\xi}) - \tilde{\boldsymbol{u}}^k(\boldsymbol{x})$ and choose $\boldsymbol{u} = \boldsymbol{u}^k$ and $\boldsymbol{v} = \tilde{\boldsymbol{u}}^k$ in Eq. 41 to find that

$$\begin{aligned}\left|\sigma_i^k(u)\right| &= \left|-\nabla PD^\epsilon(\tilde{\boldsymbol{u}}^k)(\boldsymbol{x}_i) + \nabla PD^\epsilon(\boldsymbol{u}^k)(\boldsymbol{x}_i)\right| \\ &\leq \frac{2C_2}{\epsilon\omega_d}\left|\int_{H_1(\mathbf{0})} J(|\boldsymbol{\xi}|)\frac{\left|\boldsymbol{u}^k(\boldsymbol{x}_i+\epsilon\boldsymbol{\xi})-\tilde{\boldsymbol{u}}^k(\boldsymbol{x}_i+\epsilon\boldsymbol{\xi})-(\boldsymbol{u}^k(\boldsymbol{x}_i)-\tilde{\boldsymbol{u}}^k(\boldsymbol{x}_i))\right|}{\epsilon\,|\boldsymbol{\xi}|}d\boldsymbol{\xi}\right|.\end{aligned} \tag{42}$$

Here C_2 is the maximum of the second derivative of the profile describing the potential given by Eq. 36. Following the earlier analysis (see Eq. 26), we find that

$$\begin{aligned}\left|\boldsymbol{u}^k(\boldsymbol{x}_i+\epsilon\boldsymbol{\xi}) - \tilde{\boldsymbol{u}}^k(\boldsymbol{x}_i+\epsilon\boldsymbol{\xi})\right| &\leq c^\gamma h^\gamma \sup_t \|\boldsymbol{u}(t)\|_{C^{0,\gamma}(D;\mathbb{R}^d)} \\ \left|\boldsymbol{u}^k(\boldsymbol{x}_i) - \tilde{\boldsymbol{u}}^k(\boldsymbol{x}_i)\right| &\leq c^\gamma h^\gamma \sup_t \|\boldsymbol{u}(t)\|_{C^{0,\gamma}(D;\mathbb{R}^d)}.\end{aligned}$$

For reference, we define the constant

$$\bar{C} = \frac{C_2}{\omega_d}\int_{H_1(\mathbf{0})} J(|\boldsymbol{\xi}|)\frac{1}{|\boldsymbol{\xi}|}d\boldsymbol{\xi}. \tag{43}$$

We now focus on Eq. 42. We substitute the above two inequalities to get

$$\begin{aligned}\left|\sigma_i^k(u)\right| &\leq \frac{2C_2}{\epsilon^2\omega_d}\left|\int_{H_1(\mathbf{0})} J(|\boldsymbol{\xi}|)\frac{1}{|\boldsymbol{\xi}|}\right. \\ &\qquad \left.\left(\left|\boldsymbol{u}^k(\boldsymbol{x}_i+\epsilon\boldsymbol{\xi})-\tilde{\boldsymbol{u}}^k(\boldsymbol{x}_i+\epsilon\boldsymbol{\xi})\right| + \left|\boldsymbol{u}^k(\boldsymbol{x}_i)-\tilde{\boldsymbol{u}}^k(\boldsymbol{x}_i)\right|\right)d\boldsymbol{\xi}\right| \\ &\leq 4h^\gamma c^\gamma \frac{\bar{C}}{\epsilon^2}\sup_t \|\boldsymbol{u}(t)\|_{C^{0,\gamma}(D;\mathbb{R}^d)}.\end{aligned}$$

Therefore, we have

$$\left\|\sigma^k(u)\right\|_{L^2(D;\mathbb{R}^d)} \leq h^\gamma\left(4c^\gamma\sqrt{|D|}\frac{\bar{C}}{\epsilon^2}\sup_t \|\boldsymbol{u}(t)\|_{C^{0,\gamma}(D;\mathbb{R}^d)}\right).$$

This completes the proof of consistency of numerical approximation.

Stability

Let e^k be the total error at the kth time step. It is defined as

$$e^k := \left\| \boldsymbol{e}^k(u) \right\|_{L^2(D;\mathbb{R}^d)} + \left\| \boldsymbol{e}^k(v) \right\|_{L^2(D;\mathbb{R}^d)}.$$

To simplify the calculations, we define new term τ as

$$\tau := \sup_t \Big(\left\| \tau^k(u) \right\|_{L^2(D;\mathbb{R}^d)} + \left\| \tau^k(v) \right\|_{L^2(D;\mathbb{R}^d)} + \left\| \sigma^k(u) \right\|_{L^2(D;\mathbb{R}^d)} + \left\| \sigma^k(v) \right\|_{L^2(D;\mathbb{R}^d)} \Big).$$

From our consistency analysis, we know that to leading order

$$\tau \leq C_t \Delta t + \frac{C_s}{\epsilon^2} h^\gamma \tag{44}$$

where,

$$C_t := \frac{1}{2} \sup_t \left\| \frac{\partial^2 \boldsymbol{u}(t)}{\partial t^2} \right\|_{L^2(D;\mathbb{R}^d)} + \frac{1}{2} \sup_t \left\| \frac{\partial^3 \boldsymbol{u}(t)}{\partial t^3} \right\|_{L^2(D;\mathbb{R}^d)}, \tag{45}$$

$$C_s := c^\gamma \sqrt{|D|} \left[\epsilon^2 \sup_t \left\| \frac{\partial^2 \boldsymbol{u}(t)}{\partial t^2} \right\|_{C^{0,\gamma}(D;\mathbb{R}^d)} + 4\bar{C} \sup_t \| \boldsymbol{u}(t) \|_{C^{0,\gamma}(D;\mathbb{R}^d)} \right]. \tag{46}$$

We take L^2 norm of Eqs. 27 and 34 and add them. Noting the definition of τ as above, we get

$$e^{k+1} \leq e^k + \Delta t \left\| \boldsymbol{e}^{k+1}(v) \right\|_{L^2(D;\mathbb{R}^d)} + \Delta t \tau + \Delta t \left(\sum_i h^d \left| -\nabla PD^\epsilon(\hat{\boldsymbol{u}}^k)(\boldsymbol{x}_i) + \nabla PD^\epsilon(\tilde{\boldsymbol{u}}^k)(\boldsymbol{x}_i) \right|^2 \right)^{1/2}. \tag{47}$$

We only need to estimate the last term in the above equation. Similar to the Eq. 42, we have

$$\begin{aligned}
&\left| -\nabla PD^\epsilon(\hat{\boldsymbol{u}}^k)(\boldsymbol{x}_i) + \nabla PD^\epsilon(\tilde{\boldsymbol{u}}^k)(\boldsymbol{x}_i) \right| \\
&\leq \frac{2C_2}{\epsilon^2 \omega_d} \left| \int_{H_1(\mathbf{0})} J(|\boldsymbol{\xi}|) \frac{1}{|\boldsymbol{\xi}|} \left| \hat{\boldsymbol{u}}^k(\boldsymbol{x}_i + \epsilon\boldsymbol{\xi}) - \tilde{\boldsymbol{u}}^k(\boldsymbol{x}_i + \epsilon\boldsymbol{\xi}) - (\hat{\boldsymbol{u}}^k(\boldsymbol{x}_i) - \tilde{\boldsymbol{u}}^k(\boldsymbol{x}_i)) \right| d\boldsymbol{\xi} \right| \\
&= \frac{2C_2}{\epsilon^2 \omega_d} \left| \int_{H_1(\mathbf{0})} J(|\boldsymbol{\xi}|) \frac{1}{|\boldsymbol{\xi}|} \left| \boldsymbol{e}^k(u)(\boldsymbol{x}_i + \epsilon\boldsymbol{\xi}) - \boldsymbol{e}^k(u)(\boldsymbol{x}_i) \right| d\boldsymbol{\xi} \right| \\
&\leq \frac{2C_2}{\epsilon^2 \omega_d} \left| \int_{H_1(\mathbf{0})} J(|\boldsymbol{\xi}|) \frac{1}{|\boldsymbol{\xi}|} \left(\left| \boldsymbol{e}^k(u)(\boldsymbol{x}_i + \epsilon\boldsymbol{\xi}) \right| + \left| \boldsymbol{e}^k(u)(\boldsymbol{x}_i) \right| \right) d\boldsymbol{\xi} \right|.
\end{aligned}$$

By $\boldsymbol{e}^k(u)(\boldsymbol{x})$ we mean evaluation of piecewise extension of set $\{\boldsymbol{e}_i^k(u)\}_i$ at $\boldsymbol{x}$. We proceed further as follows

$$\begin{aligned}
&\left|-\nabla PD^\epsilon(\hat{\boldsymbol{u}}^k)(\boldsymbol{x}_i) + \nabla PD^\epsilon(\tilde{\boldsymbol{u}}^k)(\boldsymbol{x}_i)\right|^2 \\
&\leq \left(\frac{2C_2}{\epsilon^2\omega_d}\right)^2 \int_{H_1(\mathbf{0})}\int_{H_1(\mathbf{0})} J(|\boldsymbol{\xi}|)J(|\boldsymbol{\eta}|)\frac{1}{|\boldsymbol{\xi}|}\frac{1}{|\boldsymbol{\eta}|} \\
&\quad \left(\left|\boldsymbol{e}^k(u)(\boldsymbol{x}_i+\epsilon\boldsymbol{\xi})\right| + \left|\boldsymbol{e}^k(u)(\boldsymbol{x}_i)\right|\right)\left(\left|\boldsymbol{e}^k(u)(\boldsymbol{x}_i+\epsilon\boldsymbol{\eta})\right| + \left|\boldsymbol{e}^k(u)(\boldsymbol{x}_i)\right|\right) d\boldsymbol{\xi}\, d\boldsymbol{\eta}.
\end{aligned}$$

Using inequality $|ab| \leq (|a|^2 + |b|^2)/2$, we get

$$\begin{aligned}
&\left(\left|\boldsymbol{e}^k(u)(\boldsymbol{x}_i+\epsilon\boldsymbol{\xi})\right| + \left|\boldsymbol{e}^k(u)(\boldsymbol{x}_i)\right|\right)\left(\left|\boldsymbol{e}^k(u)(\boldsymbol{x}_i+\epsilon\boldsymbol{\eta})\right| + \left|\boldsymbol{e}^k(u)(\boldsymbol{x}_i)\right|\right) \\
&\leq 3\left(\left|\boldsymbol{e}^k(u)(\boldsymbol{x}_i+\epsilon\boldsymbol{\xi})\right|^2 + \left|\boldsymbol{e}^k(u)(\boldsymbol{x}_i+\epsilon\boldsymbol{\eta})\right|^2 + \left|\boldsymbol{e}^k(u)(\boldsymbol{x}_i)\right|^2\right),
\end{aligned}$$

and

$$\begin{aligned}
&\sum_{\boldsymbol{x}_i\in D} h^d \left|-\nabla PD^\epsilon(\hat{\boldsymbol{u}}^k)(\boldsymbol{x}_i) + \nabla PD^\epsilon(\tilde{\boldsymbol{u}}^k)(\boldsymbol{x}_i)\right|^2 \\
&\leq \left(\frac{2C_2}{\epsilon^2\omega_d}\right)^2 \int_{H_1(\mathbf{0})}\int_{H_1(\mathbf{0})} J(|\boldsymbol{\xi}|)J(|\boldsymbol{\eta}|)\frac{1}{|\boldsymbol{\xi}|}\frac{1}{|\boldsymbol{\eta}|} \\
&\quad \sum_{\boldsymbol{x}_i\in D} h^d 3\left(\left|\boldsymbol{e}^k(u)(\boldsymbol{x}_i+\epsilon\boldsymbol{\xi})\right|^2 + \left|\boldsymbol{e}^k(u)(\boldsymbol{x}_i+\epsilon\boldsymbol{\eta})\right|^2 + \left|\boldsymbol{e}^k(u)(\boldsymbol{x}_i)\right|^2\right) d\boldsymbol{\xi}\, d\boldsymbol{\eta}.
\end{aligned}$$

Since $\boldsymbol{e}^k(u)(\boldsymbol{x}) = \sum_{\boldsymbol{x}_i\in D} \boldsymbol{e}_i^k(u)\chi_{U_i}(\boldsymbol{x})$, we have

$$\sum_{\boldsymbol{x}_i\in D} h^d \left|-\nabla PD^\epsilon(\hat{\boldsymbol{u}}^k)(\boldsymbol{x}_i) + \nabla PD^\epsilon(\tilde{\boldsymbol{u}}^k)(\boldsymbol{x}_i)\right|^2 \leq \frac{(6\bar{C})^2}{\epsilon^4}\left\|\boldsymbol{e}^k(u)\right\|^2_{L^2(D;\mathbb{R}^d)}. \quad (48)$$

where $\bar{C}$ is given by Eq. 43. In summary Eq. 48 shows the Lipschitz continuity of the peridynamic force with respect to the L^2 norm (see Eq. 16) expressed in this context as

$$\|\nabla PD^\epsilon(\hat{\boldsymbol{u}}^k)(\boldsymbol{x}) - \nabla PD^\epsilon(\tilde{\boldsymbol{u}}^k)\|_{L^2(D;\mathbb{R}^d)} \leq \frac{(6\bar{C})}{\epsilon^2}\|\boldsymbol{e}^k(u)\|_{L^2(D;\mathbb{R}^d)}. \quad (49)$$

Finally, we substitute above inequality in Eq. 47 to get

$$e^{k+1} \leq e^k + \Delta t\left\|\boldsymbol{e}^{k+1}(v)\right\|_{L^2(D;\mathbb{R}^d)} + \Delta t\,\tau + \Delta t\frac{6\bar{C}}{\epsilon^2}\left\|\boldsymbol{e}^k(u)\right\|_{L^2(D;\mathbb{R}^d)}$$

We add positive quantity $\Delta t||e^{k+1}(u)||_{L^2(D;\mathbb{R}^d)} + \Delta t 6\bar{C}/\epsilon^2||e^k(v)||_{L^2(D;\mathbb{R}^d)}$ to the right side of above equation to get

$$e^{k+1} \leq (1 + \Delta t 6\bar{C}/\epsilon^2)e^k + \Delta t e^{k+1} + \Delta t \tau$$
$$\Rightarrow e^{k+1} \leq \frac{(1 + \Delta t 6\bar{C}/\epsilon^2)}{1 - \Delta t} e^k + \frac{\Delta t}{1 - \Delta t}\tau.$$

We recursively substitute e^j on above as follows

$$\begin{aligned} e^{k+1} &\leq \frac{(1 + \Delta t 6\bar{C}/\epsilon^2)}{1 - \Delta t} e^k + \frac{\Delta t}{1 - \Delta t}\tau \\ &\leq \left(\frac{(1 + \Delta t 6\bar{C}/\epsilon^2)}{1 - \Delta t}\right)^2 e^{k-1} + \frac{\Delta t}{1 - \Delta t}\tau \left(1 + \frac{(1 + \Delta t 6\bar{C}/\epsilon^2)}{1 - \Delta t}\right) \\ &\leq \ldots \\ &\leq \left(\frac{(1 + \Delta t 6\bar{C}/\epsilon^2)}{1 - \Delta t}\right)^{k+1} e^0 + \frac{\Delta t}{1 - \Delta t}\tau \sum_{j=0}^{k} \left(\frac{(1 + \Delta t 6\bar{C}/\epsilon^2)}{1 - \Delta t}\right)^{k-j} . \end{aligned} \tag{50}$$

Since $1/(1 - \Delta t) = 1 + \Delta t + \Delta t^2 + O(\Delta t^3)$, we have

$$\frac{(1 + \Delta t 6\bar{C}/\epsilon^2)}{1 - \Delta t} \leq 1 + (1 + 6\bar{C}/\epsilon^2)\Delta t + (1 + 6\bar{C}/\epsilon^2)\Delta t^2 + O(\bar{C}/\epsilon^2)O(\Delta t^3).$$

Now, for any $k \leq T/\Delta t$, using identity $(1 + a)^k \leq \exp[ka]$ for $a \leq 0$, we have

$$\begin{aligned} &\left(\frac{1 + \Delta t 6\bar{C}/\epsilon^2}{1 - \Delta t}\right)^k \\ &\leq \exp\left[k(1 + 6\bar{C}/\epsilon^2)\Delta t + k(1 + 6\bar{C}/\epsilon^2)\Delta t^2 + kO(\bar{C}/\epsilon^2)O(\Delta t^3)\right] \\ &\leq \exp\left[T(1 + 6\bar{C}/\epsilon^2) + T(1 + 6\bar{C}/\epsilon^2)\Delta t + O(T\bar{C}/\epsilon^2)O(\Delta t^2)\right]. \end{aligned}$$

We write above equation in more compact form as follows

$$\begin{aligned} &\left(\frac{1 + \Delta t 6\bar{C}/\epsilon^2}{1 - \Delta t}\right)^k \\ &\leq \exp\left[T(1 + 6\bar{C}/\epsilon^2)(1 + \Delta t + O(\Delta t^2))\right]. \end{aligned}$$

We use above estimate in Eq. 50 and get the following inequality for e^k

$$
\begin{aligned}
e^{k+1} &\le \exp\left[T(1+6\bar{C}/\epsilon^2)(1+\Delta t + O(\Delta t^2))\right]\left(e^0 + (k+1)\tau\Delta t/(1-\Delta t)\right) \\
&\le \exp\left[T(1+6\bar{C}/\epsilon^2)(1+\Delta t + O(\Delta t^2))\right]\left(e^0 + T\tau(1+\Delta t + O(\Delta t^2)\right).
\end{aligned}
$$

where we used the fact that $1/(1-\Delta t) = 1 + \Delta t + O(\Delta t^2)$.

Assuming the error in initial data is zero, i.e., $e^0 = 0$, and noting the estimate of τ in Eq. 44, we have

$$
\sup_k e^k \le \exp\left[T(1+6\bar{C}/\epsilon^2)\right] T\tau
$$

and we conclude to leading order that

$$
\sup_k e^k \le \exp\left[T(1+6\bar{C}/\epsilon^2)\right] T\left[C_t\Delta t + (C_s/\epsilon^2)h^\gamma\right], \tag{51}
$$

Here the constants C_t and C_s are given by Eqs. 45 and 46.This shows the stability of the numerical scheme and Theorem 2 is proved.

Stability of the Energy for the Semi-discrete Approximation

We first spatially discretize the peridynamics equation (Eq. 6). Let $\{\hat{\boldsymbol{u}}_i(t)\}_{i,\boldsymbol{x}_i\in D}$ denote the semi-discrete approximate solution which satisfies the following, for all $t \in [0,T]$ and i such that $\boldsymbol{x}_i \in D$,

$$
\ddot{\hat{\boldsymbol{u}}}_i(t) = -\nabla PD^\epsilon(\hat{\boldsymbol{u}}(t))(\boldsymbol{x}_i) + \boldsymbol{b}_i(t) \tag{52}
$$

where $\hat{\boldsymbol{u}}(t)$ is the piecewise constant extension of discrete set $\{\hat{\boldsymbol{u}}_i(t)\}_i$ and is defined as

$$
\hat{\boldsymbol{u}}(t,\boldsymbol{x}) := \sum_{i,\boldsymbol{x}_i\in D} \hat{\boldsymbol{u}}_i(t)\chi_{U_i}(\boldsymbol{x}). \tag{53}
$$

The scheme is complemented with the discretized initial conditions $\hat{\boldsymbol{u}}_i(0) = \boldsymbol{u}_0(\boldsymbol{x}_i)$ and $\hat{\boldsymbol{v}}_i(0) = \boldsymbol{v}_0(\boldsymbol{x}_i)$. We apply boundary condition by setting $\hat{\boldsymbol{u}}_i(t) = \boldsymbol{0}$ for all t and for all $\boldsymbol{x}_i \notin D$.

We have the stability of semi-discrete evolution.

Theorem 3 (Energy stability of the semi-discrete approximation). *Let $\{\hat{\boldsymbol{u}}_i(t)\}_i$ satisfy Eq. 52 and $\hat{\boldsymbol{u}}(t)$ is its piecewise constant extension. Similarily let $\hat{\boldsymbol{b}}(t,\boldsymbol{x})$ denote the piecewise constant extension of $\{\boldsymbol{b}(t,\boldsymbol{x}_i)\}_{i,\boldsymbol{x}_i\in D}$. Then the peridynamic energy $\mathcal{E}^\epsilon$ as defined in Eq. 11 satisfies, $\forall t \in [0,T]$,*

$$
\mathcal{E}^\epsilon(\hat{\boldsymbol{u}})(t) \le \left(\sqrt{\mathcal{E}^\epsilon(\hat{\boldsymbol{u}})(0)} + \frac{TC}{\epsilon^{3/2}} + \int_0^T ||\hat{\boldsymbol{b}}(s)||_{L^2(D;\mathbb{R}^d)} ds\right)^2. \tag{54}
$$

The constant C, defined in Eq. 59, is independent of ϵ and h.

Proof. We multiply Eq. 52 by $\chi_{U_i}(\boldsymbol{x})$ and sum over i and use definition of piecewise constant extension in Eq. 53 to get

$$\begin{aligned}\ddot{\hat{\boldsymbol{u}}}(t,\boldsymbol{x}) &= -\nabla P\hat{D}^{\epsilon}(\hat{\boldsymbol{u}}(t))(\boldsymbol{x}) + \hat{\boldsymbol{b}}(t,\boldsymbol{x}) \\ &= -\nabla PD^{\epsilon}(\hat{\boldsymbol{u}}(t))(\boldsymbol{x}) + \hat{\boldsymbol{b}}(t,\boldsymbol{x}) \\ &\quad + (-\nabla P\hat{D}^{\epsilon}(\hat{\boldsymbol{u}}(t))(\boldsymbol{x}) + \nabla PD^{\epsilon}(\hat{\boldsymbol{u}}(t))(\boldsymbol{x}))\end{aligned}$$

where $-\nabla P\hat{D}^{\epsilon}(\hat{\boldsymbol{u}}(t))(\boldsymbol{x})$ and $\hat{\boldsymbol{b}}(t,\boldsymbol{x})$ are given by

$$\begin{aligned}-\nabla P\hat{D}^{\epsilon}(\hat{\boldsymbol{u}}(t))(\boldsymbol{x}) &= \sum_{i,\boldsymbol{x}_i\in D} (-\nabla PD^{\epsilon}(\hat{\boldsymbol{u}}(t))(\boldsymbol{x}_i))\chi_{U_i}(\boldsymbol{x}) \\ \hat{\boldsymbol{b}}(t,\boldsymbol{x}) &= \sum_{i,\boldsymbol{x}_i\in D} \boldsymbol{b}(t,\boldsymbol{x}_i)\chi_{U_i}(\boldsymbol{x}).\end{aligned}$$

We define set as follows

$$\sigma(t,\boldsymbol{x}) := -\nabla P\hat{D}^{\epsilon}(\hat{\boldsymbol{u}}(t))(\boldsymbol{x}) + \nabla PD^{\epsilon}(\hat{\boldsymbol{u}}(t))(\boldsymbol{x}). \tag{55}$$

We use the following result which we will show after few steps

$$||\sigma(t)||_{L^2(D;\mathbb{R}^d)} \leq \frac{C}{\epsilon^{3/2}}. \tag{56}$$

We then have

$$\ddot{\hat{\boldsymbol{u}}}(t,\boldsymbol{x}) = -\nabla PD^{\epsilon}(\hat{\boldsymbol{u}}(t))(\boldsymbol{x}) + \hat{\boldsymbol{b}}(t,\boldsymbol{x}) + \sigma(t,\boldsymbol{x}). \tag{57}$$

Multiply above with $\dot{\hat{\boldsymbol{u}}}(t)$ and integrate over D to get

$$\begin{aligned}(\ddot{\hat{\boldsymbol{u}}}(t),\dot{\hat{\boldsymbol{u}}}(t)) &= (-\nabla PD^{\epsilon}(\hat{\boldsymbol{u}}(t)),\dot{\hat{\boldsymbol{u}}}(t)) \\ &\quad + (\hat{\boldsymbol{b}}(t),\dot{\hat{\boldsymbol{u}}}(t)) + (\sigma(t),\dot{\hat{\boldsymbol{u}}}(t)).\end{aligned}$$

Consider energy $\mathcal{E}^{\epsilon}(\hat{\boldsymbol{u}})(t)$ given by Eq. 11 and note the identity Eq. 12, to have

$$\begin{aligned}\frac{d}{dt}\mathcal{E}^{\epsilon}(\hat{\boldsymbol{u}})(t) &= (\hat{\boldsymbol{b}}(t),\dot{\hat{\boldsymbol{u}}}(t)) + (\sigma(t),\dot{\hat{\boldsymbol{u}}}(t)) \\ &\leq \left(||\hat{\boldsymbol{b}}(t)||_{L^2(D;\mathbb{R}^d)} + ||\sigma(t)||_{L^2(D;\mathbb{R}^d)}\right)||\dot{\hat{\boldsymbol{u}}}(t)||_{L^2(D;\mathbb{R}^d)},\end{aligned}$$

where we used Hölder inequality in last step. Since $PD^{\epsilon}(\boldsymbol{u})$ is positive for any $\boldsymbol{u}$, we have

$$||\dot{\hat{\boldsymbol{u}}}(t)|| \leq 2\sqrt{\frac{1}{2}||\dot{\hat{\boldsymbol{u}}}(t)||^2_{L^2(D;\mathbb{R}^d)} + PD^\epsilon(\hat{\boldsymbol{u}}(t))} = 2\sqrt{\mathcal{E}^\epsilon(\hat{\boldsymbol{u}})(t)}.$$

Using above, we get

$$\frac{1}{2}\frac{d}{dt}\mathcal{E}^\epsilon(\hat{\boldsymbol{u}})(t) \leq \left(||\hat{\boldsymbol{b}}(t)||_{L^2(D;\mathbb{R}^d)} + ||\sigma(t)||_{L^2(D;\mathbb{R}^d)}\right)\sqrt{\mathcal{E}^\epsilon(\hat{\boldsymbol{u}})(t)}.$$

Let $\delta > 0$ be some arbitrary but fixed real number and let $A(t) = \delta + \mathcal{E}^\epsilon(\hat{\boldsymbol{u}})(t)$. Then

$$\frac{1}{2}\frac{d}{dt}A(t) \leq \left(||\hat{\boldsymbol{b}}(t)||_{L^2(D;\mathbb{R}^d)} + ||\sigma(t)||_{L^2(D;\mathbb{R}^d)}\right)\sqrt{A(t)}.$$

Using the fact that $\frac{1}{\sqrt{A(t)}}\frac{d}{dt}A(t) = 2\frac{d}{dt}\sqrt{A(t)}$, we have

$$\begin{aligned}\sqrt{A(t)} &\leq \sqrt{A(0)} + \int_0^t \left(||\hat{\boldsymbol{b}}(s)||_{L^2(D;\mathbb{R}^d)} + ||\sigma(s)||_{L^2(D;\mathbb{R}^d)}\right) ds \\ &\leq \sqrt{A(0)} + \frac{TC}{\epsilon^{3/2}} + \int_0^T ||\hat{\boldsymbol{b}}(s)||_{L^2(D;\mathbb{R}^d)} ds.\end{aligned}$$

where we used bound on $||\sigma(s)||_{L^2(D;\mathbb{R}^d)}$ from Eq. 56. Noting that $\delta > 0$ is arbitrary, we send it to zero to get

$$\sqrt{\mathcal{E}^\epsilon(\hat{\boldsymbol{u}})(t)} \leq \sqrt{\mathcal{E}^\epsilon(\hat{\boldsymbol{u}})(0)} + \frac{TC}{\epsilon^{3/2}} + \int_0^T ||\hat{\boldsymbol{b}}(s)|| ds,$$

and Eq. 54 follows by taking square of above equation.

It remains to show in Eq. 56. To simplify the calculations, we use the following notations: let $\boldsymbol{\xi} \in H_1(\boldsymbol{0})$ and let

$$\begin{aligned} s_{\boldsymbol{\xi}} &= \epsilon|\boldsymbol{\xi}|, e_{\boldsymbol{\xi}} = \frac{\boldsymbol{\xi}}{|\boldsymbol{\xi}|}, \bar{\omega}(\boldsymbol{x}) = \omega(\boldsymbol{x})\omega(\boldsymbol{x} + \epsilon\boldsymbol{\xi}), \\ S_{\boldsymbol{\xi}}(\boldsymbol{x}) &= \frac{\hat{\boldsymbol{u}}(t, \boldsymbol{x} + \epsilon\boldsymbol{\xi}) - \hat{\boldsymbol{u}}(t, \boldsymbol{x})}{s_{\boldsymbol{\xi}}} \cdot e_{\boldsymbol{\xi}}. \end{aligned}$$

With above notations and using expression of $-\nabla PD^\epsilon$ from Eq. 38, we have for $\boldsymbol{x} \in U_i$

$$\begin{aligned} |\sigma(t, \boldsymbol{x})| &= |-\nabla PD^\epsilon(\hat{\boldsymbol{u}}(t))(\boldsymbol{x}_i) + \nabla PD^\epsilon(\hat{\boldsymbol{u}}(t))(\boldsymbol{x})| \\ &= \left|\frac{2}{\epsilon\omega_d}\int_{H_1(\boldsymbol{0})} \frac{J(|\boldsymbol{\xi}|)}{\sqrt{s_{\boldsymbol{\xi}}}} \left(\bar{\omega}(\boldsymbol{x}_i)F_1'(\sqrt{s_{\boldsymbol{\xi}}}S_{\boldsymbol{\xi}}(\boldsymbol{x}_i)) - \bar{\omega}(\boldsymbol{x})F_1'(\sqrt{s_{\boldsymbol{\xi}}}S_{\boldsymbol{\xi}}(\boldsymbol{x}))\right) e_{\boldsymbol{\xi}} d\boldsymbol{\xi}\right| \end{aligned}$$

$$
\begin{aligned}
&\leq \frac{2}{\epsilon \omega_d} \int_{H_1(\mathbf{0})} \frac{J(|\boldsymbol{\xi}|)}{\sqrt{s_\xi}} \left| \bar{\omega}(\boldsymbol{x}_i) F_1'(\sqrt{s_\xi} S_\xi(\boldsymbol{x}_i)) - \bar{\omega}(\boldsymbol{x}) F_1'(\sqrt{s_\xi} S_\xi(\boldsymbol{x})) \right| d\boldsymbol{\xi} \\
&\leq \frac{2}{\epsilon \omega_d} \int_{H_1(\mathbf{0})} \frac{J(|\boldsymbol{\xi}|)}{\sqrt{s_\xi}} \left(\left| \bar{\omega}(\boldsymbol{x}_i) F_1'(\sqrt{s_\xi} S_\xi(\boldsymbol{x}_i)) \right| + \left| \bar{\omega}(\boldsymbol{x}) F_1'(\sqrt{s_\xi} S_\xi(\boldsymbol{x})) \right| \right) d\boldsymbol{\xi}.
\end{aligned}
\tag{58}
$$

Using the fact that $0 \leq \omega(\boldsymbol{x}) \leq 1$ and $|F_1'(r)| \leq C_1$, where C_1 is $\sup_r |F_1'(r)|$, we get

$$
|\sigma(t, \boldsymbol{x})| \leq \frac{4 C_1 \bar{J}_{1/2}}{\epsilon^{3/2}}.
$$

where $\bar{J}_{1/2} = (1/\omega_d) \int_{H_1(\mathbf{0})} J(|\boldsymbol{\xi}|)|\boldsymbol{\xi}|^{-1/2} d\boldsymbol{\xi}$.

Taking the L^2 norm of $\sigma(t, \boldsymbol{x})$, we get

$$
||\sigma(t)||^2_{L^2(D;\mathbb{R}^d)} = \sum_{i, \boldsymbol{x}_i \in D} \int_{U_i} |\sigma(t, \boldsymbol{x})|^2 d\boldsymbol{x} \leq \left(\frac{4 C_1 \bar{J}_{1/2}}{\epsilon^{3/2}} \right)^2 \sum_{i, \boldsymbol{x}_i \in D} \int_{U_i} d\boldsymbol{x}
$$

thus

$$
||\sigma(t)||_{L^2(D;\mathbb{R}^d)} \leq \frac{4 C_1 \bar{J}_{1/2} \sqrt{|D|}}{\epsilon^{3/2}} = \frac{C}{\epsilon^{3/2}}
$$

where

$$
C := 4 C_1 \bar{J}_{1/2} \sqrt{|D|}. \tag{59}
$$

This completes the proof.

Finite Element Approximation

Let V_h be the approximation of $H_0^2(D, \mathbb{R}^d)$ associated with linear continuous interpolation associated with the mesh $\mathcal{T}_h$ (triangular or tetrahedral) where h denotes the size of finite element mesh. Let $\mathcal{I}_h(u)$ be defined as below

$$
\mathcal{I}_h(u)(x) = \sum_{T \in \mathcal{T}_h} \left[\sum_{i \in N_T} u(x_i) \phi_i(x) \right]
$$

where N_T is the set of global indices of nodes associated to finite element T, ϕ_i is the linear interpolation function associated to node i, and x_i is the material coordinate of node i.

Assuming that the size of each element in the mesh $\mathcal{T}_h$ is bounded by h, we have (see, e.g., [Theorem 4.6, Arnold 2011])

$$||u - \mathcal{I}_h(u)|| \leq ch^2||u||_2, \qquad \forall u \in H_0^2(D; \mathbb{R}^d). \tag{60}$$

Projection of Function in FE Space

Let $r_h(u) \in V_h$ be the projection of $u \in H_0^2(D; \mathbb{R}^d)$. It is defined as

$$||u - r_h(u)|| = \inf_{\tilde{u} \in V_h} ||u - \tilde{u}||. \tag{61}$$

It also satisfies the following

$$(r_h(u), \tilde{u}) = (u, \tilde{u}), \qquad \forall \tilde{u} \in V_h. \tag{62}$$

Since $\mathcal{I}_h(u) \in V_h$, we get an upper bound on right-hand side term and we have

$$||u - r_h(u)|| \leq ch^2||u||_2 \qquad \forall u \in H_0^2(D; \mathbb{R}^d). \tag{63}$$

Semi-discrete Approximation

Let $u_h(t) \in V_h$ be the approximation of $u(t)$ which satisfies the following

$$(\ddot{u}_h, \tilde{u}) + a^\epsilon(u_h(t), \tilde{u}) = (b(t), \tilde{u}), \qquad \forall \tilde{u} \in V_h. \tag{64}$$

We now show that the semi-discrete approximation is stable, i.e., energy at time t is bounded by initial energy and work done by the body force.

Theorem 4 (Stability of the semi-discrete approximation). *The semi-discrete scheme is energetically stable and the energy $\mathcal{E}^\epsilon(u_h)(t)$, defined in (11), satisfies the following bound*

$$\mathcal{E}^\epsilon(u_h)(t) \leq \left[\sqrt{\mathcal{E}^\epsilon(u_h)(0)} + \int_0^t ||b(\tau)|| d\tau \right]^2.$$

We note that, while proving the stability of semi-discrete scheme corresponding to nonlinear peridynamics, we do not require any assumption on strain $S(y, x; u_h)$.

Proof. Letting $\tilde{u} = \dot{u}_h(t)$ in (10) and noting the identity (12), we get

$$\frac{d}{dt}\mathcal{E}^\epsilon(u_h)(t) = (b(t), \dot{u}_h(t)) \leq ||b(t)|| ||\dot{u}_h(t)||$$

We also have

$$||\dot{u}_h(t)|| \leq 2\sqrt{\frac{1}{2}||\dot{u}_h||^2 + PD^\epsilon(u_h(t))} = 2\sqrt{\mathcal{E}^\epsilon(u_h)(t)}$$

where we used the fact that $PD^\epsilon(u)(t)$ is nonnegative. We have

$$\frac{d}{dt}\mathcal{E}^\epsilon(u_h)(t) \leq 2\sqrt{\mathcal{E}^\epsilon(u_h)(t)}||b(t)||.$$

Fix $\delta > 0$ and let $A(t) = \mathcal{E}^\epsilon(u_h(t)) + \delta$. Then, from above equation, we easily have

$$\frac{d}{dt}A(t) \leq 2\sqrt{A(t)}||b(t)|| \quad \Rightarrow \frac{1}{2}\frac{\frac{d}{dt}A(t)}{\sqrt{A(t)}} \leq ||b(t)||.$$

Noting that $\frac{1}{\sqrt{a(t)}}\frac{da(t)}{dt} = 2\frac{d}{dt}\sqrt{a(t)}$, integrating from $t = 0$ to τ, and relabeling τ as t, we get

$$\sqrt{A(t)} \leq \sqrt{A(0)} + \int_0^t ||b(s)||ds.$$

Letting $\delta \to 0$ and taking the square of both sides proves the claim.

Central Difference Time Discretization

For illustration, we consider the central difference scheme and present the convergence rate for the central difference scheme for the fully nonlinear problem. We remark that the extension of these results to the general Newmark scheme is straightforward. We then consider a linearized peridynamics and demonstrate CFL-like conditions for stability of the fully discrete scheme.

Let Δt be the time step. The exact solution at $t^k = k\Delta t$ (or time step k) is denoted as (u^k, v^k), with $v^k = \partial u^k/\partial t$, and the projection onto V_h at t^k is given by $(r_h(u^k), r_h(v^k))$. The solution of the discrete problem at time step k is denoted as (u_h^k, v_h^k).

We approximate the initial data on displacement u_0 and velocity v_0 by their projection $r_h(u_0)$ and $r_h(v_0)$. Let $u_h^0 = r_h(u_0)$ and $v_h^0 = r_h(v_0)$. For $k \geq 1$, (u_h^k, v_h^k) satisfies, for all $\tilde{u} \in V_h$,

$$\left(\frac{u_h^{k+1} - u_h^k}{\Delta t}, \tilde{u}\right) = (v_h^{k+1}, \tilde{u}),$$

$$\left(\frac{v_h^{k+1} - v_h^k}{\Delta t}, \tilde{u}\right) = (-\nabla PD^\epsilon(u_h^k), \tilde{u}) + (b_h^k, \tilde{u}), \tag{65}$$

where we denote projection of $b(t^k)$, $r_h(b(t^k))$, as b_h^k. Combining the two equations delivers central difference equation for u_h^k. We have

$$\left(\frac{u_h^{k+1} - 2u_h^k + u_h^{k-1}}{\Delta t^2}, \tilde{u}\right) = (-\nabla PD^\epsilon(u_h^k), \tilde{u}) + (b_h^k, \tilde{u}), \qquad \forall \tilde{u} \in V_h. \tag{66}$$

For $k = 0$, we have $\forall \tilde{u} \in V_h$

$$\left(\frac{u_h^1 - u_h^0}{\Delta t^2}, \tilde{u}\right) = \frac{1}{2}(-\nabla PD^\epsilon(u_h^0), \tilde{u}) + \frac{1}{\Delta t}(v_h^0, \tilde{u}) + \frac{1}{2}(b_h^0, \tilde{u}). \tag{67}$$

We now show that finite element discretization converges to the exact solution.

Convergence of Approximation

In this section, we establish uniform bound on the discretization error and prove that approximate solution converges to the exact solution at the rate $C_t \Delta t + C_s h^2/\epsilon^2$ for fixed $\epsilon > 0$. We first compare the exact solution with its projection in V_h and then compare the projection with approximate solution. We further divide the calculation of error between projection and approximate solution in two parts, namely, consistency analysis and error analysis.

Error E^k is given by

$$E^k := ||u_h^k - u(t^k)|| + ||v_h^k - v(t^k)||.$$

We split the error as follows

$$E^k \leq \left(||u^k - r_h(u^k)|| + ||v^k - r_h(v^k)||\right) + \left(||r_h(u^k) - u_h^k|| + ||r_h(v^k) - v_h^k||\right),$$

where first term is error between exact solution and projections and second term is error between projections and approximate solution. Let

$$e_h^k(u) := r_h(u^k) - u_h^k \quad \text{and} \quad e_h^k(v) := r_h(v^k) - v_h^k \tag{68}$$

and

$$e^k := ||e_h^k(u)|| + ||e_h^k(v)||. \tag{69}$$

Using (63), we have

$$E^k \leq C_p h^2 + e^k, \tag{70}$$

where

$$C_p := c\left[\sup_t ||u(t)||_2 + \sup_t ||\frac{\partial u(t)}{\partial t}||_2\right]. \tag{71}$$

We have the following main result.

Theorem 5 (Convergence of the central difference approximation). *Let (u, v) be the exact solution of peridynamics equation in (6). Let (u_h^k, v_h^k) be the central difference approximation in time and piecewise linear finite element approximation in space solution of (65). If $u, v \in C^2([0, T], H_0^2(D; \mathbb{R}^d))$, then the scheme is consistent, and the error E^k satisfies the following bound*

$$\begin{aligned}
&\sup_{k \le T/\Delta t} E^k \\
&= C_p h^2 + \exp[T(1 + L/\epsilon^2)(1 + \Delta t + O(\Delta t^2))] \\
&\quad \left[e^0 + T(1 + \Delta t + O(\Delta t^2))\left(C_t \Delta t + C_s \frac{h^2}{\epsilon^2}\right)\right]
\end{aligned} \tag{72}$$

where constants C_p, C_t, and C_s are given by (71) and (79). The constant L/ϵ^2 is the Lipschitz constant of $-\nabla PD^\epsilon(u)$ in L^2 (see Theorem 1).

If the error in initial data is zero, then E^k is of the order of $C_t \Delta t + C_s h^2/\epsilon^2$.

Error Analysis

We derive the equation for evolution of $e_h^k(u)$ as follows

$$\begin{aligned}
&\left(\frac{u_h^{k+1} - u_h^k}{\Delta t} - \frac{r_h(u^{k+1}) - r_h(u^k)}{\Delta t}, \tilde{u}\right) \\
&= (v_h^{k+1}, \tilde{u}) - \left(\frac{r_h(u^{k+1}) - r_h(u^k)}{\Delta t}, \tilde{u}\right) \\
&= (v_h^{k+1}, \tilde{u}) - (r_h(v^{k+1}), \tilde{u}) + (r_h(v^{k+1}), \tilde{u}) - (v^{k+1}, \tilde{u}) \\
&\quad + (v^{k+1}, \tilde{u}) - \left(\frac{\partial u^{k+1}}{\partial t}, \tilde{u}\right) \\
&\quad + \left(\frac{\partial u^{k+1}}{\partial t}, \tilde{u}\right) - \left(\frac{u^{k+1} - u^k}{\Delta t}, \tilde{u}\right) \\
&\quad + \left(\frac{u^{k+1} - u^k}{\Delta t}, \tilde{u}\right) - \left(\frac{r_h(u^{k+1}) - r_h(u^k)}{\Delta t}, \tilde{u}\right).
\end{aligned}$$

Using property $(r_h(u), \tilde{u}) = (u, \tilde{u})$ for $\tilde{u} \in V_h$ and the fact that $\frac{\partial u(t^{k+1})}{\partial t} = v^{k+1}$ where u is the exact solution, we get

$$\left(\frac{e_h^{k+1}(u) - e_h^k(u)}{\Delta t}, \tilde{u}\right) = (e_h^{k+1}(v), \tilde{u}) + \left(\frac{\partial u^{k+1}}{\partial t}, \tilde{u}\right) - \left(\frac{u^{k+1} - u^k}{\Delta t}, \tilde{u}\right). \quad (73)$$

Let $(\tau_h^k(u), \tau_h^k(v))$ be the consistency error in time discretization given by

$$\tau_h^k(u) := \frac{\partial u^{k+1}}{\partial t} - \frac{u^{k+1} - u^k}{\Delta t},$$
$$\tau_h^k(v) := \frac{\partial v^k}{\partial t} - \frac{v^{k+1} - v^k}{\Delta t}.$$

With above notation, we have

$$(e_h^{k+1}(u), \tilde{u}) = (e_h^k(u), \tilde{u}) + \Delta t (e_h^{k+1}(v), \tilde{u}) + \Delta t (\tau_h^k(u), \tilde{u}). \quad (74)$$

We now derive the equation for $e_h^k(v)$ as follows

$$\begin{aligned}
&\left(\frac{v_h^{k+1} - v_h^k}{\Delta t} - \frac{r_h(v^{k+1}) - r_h(v^k)}{\Delta t}, \tilde{u}\right) \\
&= (-\nabla PD^\epsilon(u_h^k), \tilde{u}) + (b_h^k, \tilde{u}) - \left(\frac{r_h(v^{k+1}) - r_h(v^k)}{\Delta t}, \tilde{u}\right) \\
&= (-\nabla PD^\epsilon(u_h^k), \tilde{u}) + (b^k, \tilde{u}) - \left(\frac{\partial v^k}{\partial t}, \tilde{u}\right) \\
&\quad + \left(\frac{\partial v^k}{\partial t}, \tilde{u}\right) - \left(\frac{v^{k+1} - v^k}{\Delta t}, \tilde{u}\right) \\
&\quad + \left(\frac{v^{k+1} - v^k}{\Delta t}, \tilde{u}\right) - \left(\frac{r_h(v^{k+1}) - r_h(v^k)}{\Delta t}, \tilde{u}\right) \\
&= \left(-\nabla PD^\epsilon(u_h^k) + \nabla PD^\epsilon(u^k), \tilde{u}\right) + (b_h^k - b(t^k), \tilde{u}) \\
&\quad + \left(\frac{\partial v^k}{\partial t}, \tilde{u}\right) - \left(\frac{v^{k+1} - v^k}{\Delta t}, \tilde{u}\right) + \left(\frac{v^{k+1} - v^k}{\Delta t}, \tilde{u}\right) - \left(\frac{r_h(v^{k+1}) - r_h(v^k)}{\Delta t}, \tilde{u}\right) \\
&= \left(-\nabla PD^\epsilon(u_h^k) + \nabla PD^\epsilon(u^k), \tilde{u}\right) + \left(\frac{\partial v^k}{\partial t} - \frac{v^{k+1} - v^k}{\Delta t}, \tilde{u}\right)
\end{aligned}$$

where we used the property of $r_h(u)$ and the fact that

$$(-\nabla PD^\epsilon(u^k), \tilde{u}) + (b^k, \tilde{u}) - \left(\frac{\partial v^k}{\partial t}, \tilde{u}\right) = 0, \quad \forall \tilde{u} \in H_0^2(D; \mathbb{R}^d).$$

We further divide the error in peridynamics force as follows

$$\big(-\nabla PD^\epsilon(u_h^k) + \nabla PD^\epsilon(u^k), \tilde{u}\big)$$
$$= \big(-\nabla PD^\epsilon(u_h^k) + \nabla PD^\epsilon(r_h(u^k)), \tilde{u}\big) + \big(-\nabla PD^\epsilon(r_h(u^k)) + \nabla PD^\epsilon(u^k), \tilde{u}\big).$$

We will see in the next section that the second term is related to consistency error in spatial discretization. Therefore, we define another consistency error term $\sigma^k_{per,h}(u)$ as follows

$$\sigma^k_{per,h}(u) := -\nabla PD^\epsilon(r_h(u^k)) + \nabla PD^\epsilon(u^k). \tag{75}$$

After substituting the notations related to consistency errors, we get

$$\begin{aligned}(e_h^{k+1}(v), \tilde{u}) &= (e_h^k(v), \tilde{u}) + \Delta t(-\nabla PD^\epsilon(u_h^k) + \nabla PD^\epsilon(r_h(u^k)), \tilde{u}) \\ &\quad + \Delta t(\tau_h^k(v), \tilde{u}) + \Delta t(\sigma^k_{per,h}(u), \tilde{u}).\end{aligned} \tag{76}$$

Since u, v are C^2 in time, we can easily show

$$||\tau_h^k(u)|| \leq \Delta t \sup_t ||\frac{\partial^2 u}{\partial t^2}|| \qquad \text{and} \qquad ||\tau_h^k(v)|| \leq \Delta t \sup_t ||\frac{\partial^2 v}{\partial t^2}||.$$

To estimate $\sigma^k_{per,h}(u)$, we note the Lipschitz property of peridynamics force in L^2 norm (see Theorem 1). This leads us to

$$||\sigma^k_{per,h}(u)|| \leq \frac{L}{\epsilon^2}||u^k - r_h(u^k)|| \leq \frac{Lc}{\epsilon^2} h^2 \sup_t ||u(t)||_2, \tag{77}$$

where we have relabeled the L^2 Lipschitz constant L_1 as L.

Let τ be given by

$$\begin{aligned}\tau &:= \sup_k \Big(||\tau_h^k(u)|| + ||\tau_h^k(v)|| + ||\sigma^k_{per,h}(u)||\Big) \\ &\leq C_t \Delta t + C_s \frac{h^2}{\epsilon^2}.\end{aligned} \tag{78}$$

where

$$C_t := ||\frac{\partial^2 u}{\partial t^2}|| + ||\frac{\partial^2 v}{\partial t^2}|| \quad \text{and} \quad C_s := Lc \sup_t ||u(t)||_2. \tag{79}$$

In equation for $e_h^k(u)$ (see (74)), we take $\tilde{u} = e_h^{k+1}(u)$. Note that $e_h^{k+1}(u) = u_h^k - r_h(u^k) \in V_h$. We have

$$||e_h^{k+1}(u)||^2 = (e_h^k(u), e_h^{k+1}(u)) + \Delta t(e_h^{k+1}(v), e_h^{k+1}(u)) + \Delta t(\tau_h^k(u), e_h^{k+1}(u)).$$

Using the fact that $(u, v) \leq ||u||||v||$, we get

$$||e_h^{k+1}(u)||^2 \leq ||e_h^k(u)||||e_h^{k+1}(u)|| + \Delta t||e_h^{k+1}(v)||||e_h^{k+1}(u)|| \\ + \Delta t||\tau_h^k(u)||||e_h^{k+1}(u)||.$$

Canceling $||e_h^{k+1}(u)||$ from both sides gives

$$||e_h^{k+1}(u)|| \leq ||e_h^k(u)|| + \Delta t||e_h^{k+1}(v)|| + \Delta t||\tau_h^k(u)||. \tag{80}$$

Similarly, if we choose $\tilde{u} = e_h^{k+1}(v)$ in (76) and use the steps similar to above, we get

$$||e_h^{k+1}(v)|| \leq ||e_h^k(v)|| + \Delta t|| - \nabla PD^\epsilon(u_h^k) + \nabla PD^\epsilon(r_h(u^k))|| \\ + \Delta t \left(||\tau_h^k(v)|| + ||\sigma_{per,h}^k(u)||\right). \tag{81}$$

Using the Lipschitz property of the peridynamics force in L^2, we have

$$|| - \nabla PD^\epsilon(u_h^k) + \nabla PD^\epsilon(r_h(u^k))|| \leq \frac{L}{\epsilon^2}||u_h^k - r_h(u^k)|| = \frac{L}{\epsilon^2}||e_h^k(u)||. \tag{82}$$

After adding (80) and (81) and substituting (82), we get

$$||e_h^{k+1}(u)|| + ||e_h^{k+1}(v)|| \leq ||e_h^k(u)|| + ||e_h^k(v)|| + \Delta t||e_h^{k+1}(v)|| \\ + \frac{L}{\epsilon^2}\Delta t||e_h^k(u)|| + \Delta t\tau$$

where τ is defined in (78).

Let $e^k := ||e_h^k(u)|| + ||e_h^k(v)||$. Assuming $L/\epsilon^2 \geq 1$, we get

$$e^{k+1} \leq e^k + \Delta t e^{k+1} + \Delta t\frac{L}{\epsilon^2}e^k + \Delta t\tau$$

$$\Rightarrow e^{k+1} \leq \frac{1 + \Delta t L/\epsilon^2}{1 - \Delta t}e^k + \frac{\Delta t}{1 - \Delta t}\tau.$$

Substituting e^k recursively in above equation, we get

$$e^{k+1} \leq \left(\frac{1 + \Delta t L/\epsilon^2}{1 - \Delta t}\right)^{k+1} e^0 + \frac{\Delta t}{1 - \Delta t}\tau \sum_{j=0}^{k} \left(\frac{1 + \Delta t L/\epsilon^2}{1 - \Delta t}\right)^{k-j}.$$

Noting $1/(1 - \Delta t) = 1 + \Delta t + \Delta t^2 + O(\Delta t^3)$,

$$\frac{1+\Delta t L/\epsilon^2}{1-\Delta t} \leq 1 + (1 + L/\epsilon^2)\Delta t + (1 + L/\epsilon^2)\Delta t^2 + O(L/\epsilon^2)O(\Delta t^3),$$

and $(1 + a\Delta t)^k \leq \exp[ka\Delta t] \leq \exp[Ta]$ for $a > 0$, we get

$$\begin{aligned}\left(\frac{1+\Delta t L/\epsilon^2}{1-\Delta t}\right)^k &\leq \exp[k\Delta t(1 + L/\epsilon^2) + k\Delta t^2(1 + L/\epsilon^2) + kO(L/\epsilon^2)O(\Delta t^3)] \\ &\leq \exp[T(1 + L/\epsilon^2) + T\Delta t(1 + L/\epsilon^2) + O(TL/\epsilon^2)O(\Delta t^2)] \\ &= \exp[T(1 + L/\epsilon^2)(1 + \Delta t + O(\Delta t^2))].\end{aligned}$$

Substituting above estimates, we can easily show that

$$\begin{aligned}e^{k+1} &\leq \exp[T(1 + L/\epsilon^2)(1 + \Delta t + O(\Delta t^2))] \\ &\quad \left[e^0 + \Delta t(1 + \Delta t + O(\Delta t^2))\tau \sum_{j=0}^{k} 1\right] \\ &\leq \exp[T(1 + L/\epsilon^2)(1 + \Delta t + O(\Delta t^2))]\left[e^0 + k\Delta t(1 + \Delta t + O(\Delta t^2))\tau\right].\end{aligned}$$

Finally, we substitute above into (70) to have

$$\begin{aligned}E^k \leq C_p h^2 &+ \exp[T(1 + L/\epsilon^2)(1 + \Delta t + O(\Delta t^2))] \\ &\left[e^0 + k\Delta t(1 + \Delta t + O(\Delta t^2))\tau\right].\end{aligned}$$

After taking sup over $k \leq T/\Delta t$, we get the desired result and proof of Theorem 2 is complete.

We now consider the stability of linearized peridynamics model.

Stability Condition for Linearized Peridynamics

In this section, we linearize the peridynamics model and obtain a CFL-like stability condition. For problems where strains are small, the stability condition for the linearized model is expected to work for nonlinear model. The slope of peridynamics potential f is constant for sufficiently small strain, and therefore for small strain, the nonlinear model behaves like a linear model. When displacement field is smooth, the difference between the linearized peridynamics force and nonlinear peridynamics force is of the order of ϵ. See [Proposition 4, Jha and Lipton 2017c].

In (5), linearization gives

$$-\nabla PD_l^\epsilon(u)(x) = \frac{4}{\epsilon^{d+1}\omega_d}\int_{H_\epsilon(x)} \omega(x)\omega(y)J^\epsilon(|y-x|)f'(0)S(u)e_{y-x}dy. \quad (83)$$

The corresponding bilinear form is denoted as a_l^ϵ and is given by

$$a_l^\epsilon(u, v) = \frac{2}{\epsilon^{d+1}\omega_d} \int_D \int_{H_\epsilon(x)} \omega(x)\omega(y) J^\epsilon(|y-x|) f'(0)|y-x| S(u) S(v) dy dx. \tag{84}$$

We have

$$(-\nabla PD_l^\epsilon(u), v) = -a_l^\epsilon(u, v).$$

We now discuss the stability of the FEM approximation to the linearized problem. We replace $-\nabla PD^\epsilon$ by its linearization denoted by $-\nabla PD_l^\epsilon$ in (66) and (67). The corresponding approximate solution in V_h is denoted by $u_{l,h}^k$ where

$$\left(\frac{u_{l,h}^{k+1} - 2u_{l,h}^k + u_{l,h}^{k-1}}{\Delta t^2}, \tilde{u} \right) = (-\nabla PD_l^\epsilon(u_{l,h}^k), \tilde{u}) + (b_h^k, \tilde{u}), \qquad \forall \tilde{u} \in V_h \tag{85}$$

and

$$\left(\frac{u_{l,h}^1 - u_{l,h}^0}{\Delta t^2}, \tilde{u} \right) = \frac{1}{2}(-\nabla PD^\epsilon(u_{l,h}^0), \tilde{u}) + \frac{1}{\Delta t}(v_{l,h}^0, \tilde{u}) + \frac{1}{2}(b_h^0, \tilde{u}), \qquad \forall \tilde{u} \in V_h. \tag{86}$$

We will adopt the following notations

$$\begin{aligned} &\overline{u}_h^{k+1} := \frac{u_h^{k+1} + u_h^k}{2}, \ \overline{u}_h^k := \frac{u_h^k + u_h^{k-1}}{2}, \\ &\bar{\partial}_t u_h^k := \frac{u_h^{k+1} - u_h^{k-1}}{2\Delta t}, \ \bar{\partial}_t^+ u_h^k := \frac{u_h^{k+1} - u_h^k}{\Delta t}, \ \bar{\partial}_t^- u_h^k := \frac{u_h^k - u_h^{k-1}}{\Delta t}. \end{aligned} \tag{87}$$

With above notations, we have

$$\bar{\partial}_t u_h^k = \frac{\bar{\partial}_t^+ u_h^k + \bar{\partial}_h^- u_h^k}{2} = \frac{\overline{u}_h^{k+1} - \overline{u}_h^k}{\Delta t}.$$

We also define

$$\bar{\partial}_{tt} u_h^k := \frac{u_h^{k+1} - 2u_h^k + u_h^{k-1}}{\Delta t^2} = \frac{\bar{\partial}_t^+ u_h^k - \bar{\partial}_t^- u_h^k}{\Delta t}.$$

We introduce the discrete energy associated with $u_{l,h}^k$ at time step k as defined by

$$\mathcal{E}(u_{l,h}^k) := \frac{1}{2}\left[||\bar{\partial}_t^+ u_{l,h}^k||^2 - \frac{\Delta t^2}{4} a_l^\epsilon(\bar{\partial}_t^+ u_{l,h}^k, \bar{\partial}_t^+ u_{l,h}^k) + a_l^\epsilon(\overline{u}_{l,h}^{k+1}, \overline{u}_{l,h}^{k+1}) \right]$$

Following [Theorem 4.1, Karaa 2012], we have

Theorem 6 (Stability of the central difference approximation of linearized peridynamics).
Let $u_{l,h}^k$ be the approximate solution of (85) and (86) with respect to linearized peridynamics. In the absence of the body force $b(t) = 0$ and for all t, if Δt satisfies the CFL-like condition

$$\frac{\Delta t^2}{4} \sup_{u \in V_h \setminus \{0\}} \frac{a_l^\epsilon(u,u)}{(u,u)} \le 1, \tag{88}$$

then the discrete energy is positive and satisfies

$$\mathcal{E}(u_{l,h}^k) = \mathcal{E}(u_{l,h}^{k-1}), \tag{89}$$

and we have the stability

$$\mathcal{E}(u_{l,h}^k) = \mathcal{E}(u_{l,h}^0). \tag{90}$$

Proof. Set $b(t) = 0$. Noting that a_l^ϵ is bilinear, after adding and subtracting term $(\Delta t^2/4) a_l^\epsilon(\bar{\partial}_{tt} u_{l,h}^k, \tilde{u})$ to (85), and noting the following

$$u_{l,h}^k + \frac{\Delta t^2}{4}\bar{\partial}_{tt} u_{l,h}^k = \frac{\overline{u}_{l,h}^{k+1}}{2} + \frac{\overline{u}_{l,h}^k}{2}$$

we get

$$(\bar{\partial}_{tt} u_{l,h}^k, \tilde{u}) - \frac{\Delta t^2}{4} a_l^\epsilon(\bar{\partial}_{tt} u_{l,h}^k, \tilde{u}) + \frac{1}{2} a_l^\epsilon(\overline{u}_{l,h}^{k+1} + \overline{u}_{l,h}^k, \tilde{u}) = 0.$$

We let $\tilde{u} = \bar{\partial}_t u_{l,h}^k$, to write

$$(\bar{\partial}_{tt} u_{l,h}^k, \bar{\partial}_t u_{l,h}^k) - \frac{\Delta t^2}{4} a_l^\epsilon(\bar{\partial}_{tt} u_{l,h}^k, \bar{\partial}_t u_{l,h}^k) + \frac{1}{2} a_l^\epsilon(\overline{u}_{l,h}^{k+1} + \overline{u}_{l,h}^k, \bar{\partial}_t u_{l,h}^k) = 0.$$

It is easily shown that

$$\begin{aligned}(\bar{\partial}_{tt} u_{l,h}^k, \bar{\partial}_t u_{l,h}^k) &= \left(\frac{\bar{\partial}_t^+ u_{l,h}^k - \bar{\partial}_t^- u_{l,h}^k}{\Delta t}, \frac{\bar{\partial}_t^+ u_{l,h}^k + \bar{\partial}_t^- u_{l,h}^k}{2} \right) \\ &= \frac{1}{2\Delta t}\left[||\bar{\partial}_t^+ u_{l,h}^k||^2 - ||\bar{\partial}_t^- u_{l,h}^k||^2 \right]\end{aligned}$$

and

$$a_l^\epsilon(\bar{\partial}_{tt} u_{l,h}^k, \bar{\partial}_t u_{l,h}^k) = \frac{1}{2\Delta t}\left[a_l^\epsilon(\bar{\partial}_t^+ u_{l,h}^k, \bar{\partial}_t^+ u_{l,h}^k) - a_l^\epsilon(\bar{\partial}_t^- u_{l,h}^k, \bar{\partial}_t^- u_{l,h}^k)\right].$$

Noting that $\bar{\partial}_t u_{l,h}^k = (\overline{u}_{l,h}^{k+1} - \overline{u}_{l,h}^k)/\Delta t$, we get

$$\begin{aligned}
&\frac{1}{2\Delta t} a_l^\epsilon(\overline{u}_{l,h}^{k+1} + \overline{u}_{l,h}^k, \overline{u}_{l,h}^{k+1} - \overline{u}_{l,h}^k) \\
&= \frac{1}{2\Delta t}\left[a_l^\epsilon(\overline{u}_{l,h}^{k+1}, \overline{u}_{l,h}^{k+1}) - a_l^\epsilon(\overline{u}_{l,h}^k, \overline{u}_{l,h}^k)\right].
\end{aligned}$$

After combining the above equations, we get

$$\begin{aligned}
&\frac{1}{\Delta t}\left[\left(\frac{1}{2}||\bar{\partial}_t^+ u_{l,h}^k||^2 - \frac{\Delta t^2}{8} a_l^\epsilon(\bar{\partial}_t^+ u_{l,h}^k, \bar{\partial}_t^+ u_{l,h}^k) + \frac{1}{2} a_l^\epsilon(\overline{u}_{l,h}^{k+1}, \overline{u}_{l,h}^{k+1})\right)\right. \\
&\left. - \left(\frac{1}{2}||\bar{\partial}_t^- u_{l,h}^k||^2 - \frac{\Delta t^2}{8} a_l^\epsilon(\bar{\partial}_t^- u_{l,h}^k, \bar{\partial}_t^- u_{l,h}^k) + \frac{1}{2} a_l^\epsilon(\overline{u}_{l,h}^k, \overline{u}_{l,h}^k)\right)\right] = 0. \quad (91)
\end{aligned}$$

We recognize the first term in bracket as $\mathcal{E}(u_{l,h}^k)$. We next prove that the second term is $\mathcal{E}(u_{l,h}^{k-1})$. We substitute $k = k - 1$ in the definition of $\mathcal{E}(u_{l,h}^k)$ to get

$$\mathcal{E}(u_{l,h}^{k-1}) = \frac{1}{2}\left[||\bar{\partial}_t^+ u_{l,h}^{k-1}||^2 - \frac{\Delta t^2}{4} a_l^\epsilon(\bar{\partial}_t^+ u_{l,h}^{k-1}, \bar{\partial}_t^+ u_{l,h}^{k-1}) + a_l^\epsilon(\overline{u}_{l,h}^k, \overline{u}_{l,h}^k)\right].$$

We clearly have $\bar{\partial}_t^+ u_{l,h}^{k-1} = \frac{u_{l,h}^{k-1+1} - u_{l,h}^{k-1}}{\Delta t} = \bar{\partial}_t^- u_{l,h}^k$, and this implies that the second term in (91) is $\mathcal{E}(u_{l,h}^{k-1})$. It now follows from (91) that $\mathcal{E}(u_{l,h}^k) = \mathcal{E}(u_{l,h}^{k-1})$.

The stability condition is such that discrete energy is positive. In the definition of $\mathcal{E}(u_{l,h}^k)$, we see that the second term is negative. We now obtain a condition on the time step that insures the sum of the first two terms is positive, and this will establish the positivity of $\mathcal{E}(u_{l,h}^k)$. Let $v = \bar{\partial}_t^+ u_{l,h}^k \in V_h$, and then we require

$$||v||^2 - \frac{\Delta t^2}{4} a_l^\epsilon(v, v) \geq 0 \quad \Rightarrow \frac{\Delta t^2}{4} \frac{a_l^\epsilon(v, v)}{||v||^2} \leq 1 \quad (92)$$

Clearly if Δt satisfies

$$\frac{\Delta t^2}{4} \sup_{v \in V_h \setminus \{0\}} \frac{a_l^\epsilon(v, v)}{||v||^2} \leq 1 \quad (93)$$

then (92) is also satisfied and the discrete energy is positive. Iteration gives $\mathcal{E}(u_{l,h}^k) = \mathcal{E}(u_{l,h}^0)$ and the theorem is proved.

Conclusion

In this chapter we computed the a priori error incurred in finite element and finite difference discretizations of peridynamics. We show that for finite element approximation with linear elements, the rate of convergence is better as compared to rate of convergence of finite difference approximation. A CFL-like condition for the stability of linearized peridynamics is obtained. For the fully nonlinear problem, we find that for the semi-discrete approximation the energy at any instant is bounded by initial energy and work done by the body force.

This model has been analyzed using a quadrature-based finite element approximation in detail in Jha and Lipton (2017c) for nonlinear nonlocal models and their linearization assuming an a priori higher regularity of solutions. If one assumes more regular solutions with three continuous spatial derivatives (no cracks), then solutions of the nonlinear nonlocal model converge to those of the classical local elastodynamic model at the rate ϵ uniformly in time in the H^1 norm (see (Theorem 5, Jha and Lipton 2017c)). The numerical simulation of problems using finite differences for this model is carried out in Lipton et al. (2016) and Diehl et al. (2016). In earlier work (Tian and Du, 2014) develop a framework for asymptotically compatible finite element schemes for linear problems where the solutions of the nonlocal problem are known to converge to a unique solution of the local problem. For the problems treated there, the discrete approximations associated with asymptotically compatible schemes converge if $h \to 0$ and $\epsilon \to 0$.

For the bond-based prototypical microelastic brittle material model analyzed here, the uniqueness property for the $\epsilon = 0$ problem is much less clear. The nonlinear nonlocal model treated in this chapter is an evolution in taking values in the vector space L^2 and can be identified with a sharp fracture evolution as $\epsilon \to 0$ (see Lipton 2014, 2016). The limit evolution is shown to be an element of the vector space, the space of special functions of bounded deformation referred to as SBD. The description and properties of this vector space can be found in Ambrosio et al. (1997). Unlike the linear nonlocal models, we do not necessarily have a unique sharp fracture evolution in the $\epsilon = 0$ limit. The uniqueness of the limit evolution for the nonlocal nonlinear model is an open question and remains to be established. The issue of nonuniqueness arises as the limit evolution is not completely characterized. What is currently missing is a limiting kinetic relation relating crack growth to crack driving force. Future work will seek to account for the missing information and address the issue of uniqueness for the limit problem.

Acknowledgements This material is based upon work supported by the US Army Research Laboratory and the US Army Research Office under contract/grant number W911NF1610456.

References

A. Agwai, I. Guven, E. Madenci, Predicting crack propagation with peridynamics: a comparative study. Int. J. Fract. **171**(1), 65–78 (2011)

B. Aksoylu, T. Mengesha, Results on nonlocal boundary value problems. Numer. Funct. Anal. Optim. **31**(12), 1301–1317 (2010)

B. Aksoylu, ML Parks, Variational theory and domain decomposition for nonlocal problems. Appl. Math. Comput. **217**(14), 6498–6515 (2011)

B. Aksoylu, Z. Unlu, Conditioning analysis of nonlocal integral operators in fractional sobolev spaces. SIAM J. Numer. Anal. **52**, 653–677 (2014)

L. Ambrosio, A. Coscia, G. Dal Maso, Fine properties of functions with bounded deformation. Arch. Ration. Mech. Anal. **139**, 201–238 (1997)

D.N. Arnold, Lecture notes on numerical analysis of partial differential equations (2011), http://www.math.umn.edu/~arnold/8445/notes.pdf

E. Askari, F. Bobaru, R. Lehoucq, M. Parks, S. Silling, O. Weckner, Peridynamics for multiscale materials modeling. J Phys Conf Ser **125**, 012078 (2008). IOP Publishing

G.A. Baker, Error estimates for finite element methods for second order hyperbolic equations. SIAM J. Numer. Anal. **13**(4), 564–576 (1976)

F. Bobaru, W. Hu, The meaning, selection, and use of the peridynamic horizon and its relation to crack branching in brittle materials. Int. J. Fract. **176**(2), 215–222 (2012)

F. Bobaru, M. Yang, L.F. Alves, S.A. Silling, E. Askari, J. Xu, Convergence, adaptive refinement, and scaling in 1d peridynamics. Int. J. Numer. Meth. Eng. **77**(6), 852–877 (2009)

X. Chen, M. Gunzburger, Continuous and discontinuous finite element methods for a peridynamics model of mechanics. Comput. Meth. Appl. Mech. Eng. **200**(9), 1237–1250 (2011)

K. Dayal, Leading-order nonlocal kinetic energy in peridynamics for consistent energetics and wave dispersion. J. Mech. Phys. Solids **105**, 235–253 (2017)

P. Diehl, R. Lipton, M. Schweitzer, Numerical verification of a bond-based softening peridynamic model for small displacements: deducing material parameters from classical linear theory. Institut für Numerische Simulation Preprint, (2016)

Q. Du, M. Gunzburger, R. Lehoucq, K. Zhou, Analysis of the volume-constrained peridynamic navier equation of linear elasticity. J. Elast. **113**(2), 193–217 (2013a)

Q. Du, L. Tian, X. Zhao, A convergent adaptive finite element algorithm for nonlocal diffusion and peridynamic models. SIAM J. Numer. Anal. **51**(2), 1211–1234 (2013b)

Q. Du, K. Zhou, Mathematical analysis for the peridynamic nonlocal continuum theory. ESAIM Math. Model. Numer. Anal. **45**(2), 217–234 (2011)

Q. Du, Y. Tao, X. Tian, A peridynamic model of fracture mechanics with bond-breaking. J. Elast. (2017), https://doi.org/10.1007/s10659-017-9661-2

E. Emmrich, R.B. Lehoucq, D. Puhst, Peridynamics: a nonlocal continuum theory, in *Meshfree Methods for Partial Differential Equations VI* (Springer, Berlin/Heidelberg, 2013), pp. 45–65

E. Emmrich, O. Weckner, et al. On the well-posedness of the linear peridynamic model and its convergence towards the navier equation of linear elasticity. Commun. Math. Sci. **5**(4), 851–864 (2007)

E. Emmrich, D. Puhst, A short note on modeling damage in peridynamics. J. Elast. **123**, 245–252 (2016)

J.T. Foster, S.A. Silling, W. Chen, An energy based failure criterion for use with peridynamic states. Int. J. Multiscale Comput. Eng. 9(6), 675–688 (2011)

W. Gerstle, N. Sau, S. Silling, Peridynamic modeling of concrete structures. Nucl. Eng. Des. **237**(12), 1250–1258 (2007)

M.J. Grote, D. Schötzau, Optimal error estimates for the fully discrete interior penalty dg method for the wave equation. J. Sci. Comput. **40**(1), 257–272 (2009)

Q. Guan, M. Gunzburger, Stability and accuracy of time-stepping schemes and dispersion relations for a nonlocal wave equation. Numer. Meth. Partial Differ. Equ. **31**(2), 500–516 (2015)

Y.D. Ha, F. Bobaru, Characteristics of dynamic brittle fracture captured with peridynamics. Eng. Fract. Mech. **78**(6), 1156–1168 (2011)

P.K. Jha, R. Lipton, Finite element approximation of nonlocal fracture models (2017a). arXiv preprint arXiv:1710.07661

P.K. Jha, R. Lipton, Numerical analysis of nonlocal fracture models models in holder space (2017b). arXiv preprint arXiv:1701.02818. To appear in SIAM Journal on Numerical Analysis 2018

P.K. Jha, R. Lipton, Numerical convergence of nonlinear nonlocal continuum models to local elastodynamics (2017c). arXiv preprint arXiv:1707.00398. To appear in International Journal for Numerical Methods in Engineering 2018

S. Karaa, Stability and convergence of fully discrete finite element schemes for the acoustic wave equation. J. Appl. Math. Comput. **40**(1–2), 659–682 (2012)

R. Lipton, Dynamic brittle fracture as a small horizon limit of peridynamics. J. Elast. **117**(1), 21–50 (2014)

R. Lipton, Cohesive dynamics and brittle fracture. J. Elast. **124**(2), 143–191 (2016)

R. Lipton, S. Silling, R. Lehoucq, Complex fracture nucleation and evolution with nonlocal elastodynamics (2016). arXiv preprint arXiv:1602.00247

R. Lipton, E. Said, P. Jha, Free damage propagation with memory. Journal of Elasticity, 1–25 (2018), https://doi.org/10.1007/s10659-018-9672

D.J. Littlewood, Simulation of dynamic fracture using peridynamics, finite element modeling, and contact, in *Proceedings of the ASME 2010 International Mechanical Engineering Congress and Exposition (IMECE)* (2010)

R.W. Macek, S.A. Silling, Peridynamics via finite element analysis. Finite Elem. Anal. Des. **43**(15), 1169–1178 (2007)

T. Mengesha, Q. Du, Analysis of a scalar peridynamic model with a sign changing kernel. Discrete Contin. Dynam. Syst. B **18**, 1415–1437 (2013)

T. Mengesha, Q. Du, Nonlocal constrained value problems for a linear peridynamic navier equation. J. Elast. **116**(1), 27–51 (2014)

S. Silling, O. Weckner, E. Askari, F. Bobaru, Crack nucleation in a peridynamic solid. Int. J. Fract. **162**(1–2), 219–227 (2010)

S.A. Silling, Reformulation of elasticity theory for discontinuities and long-range forces. J. Mech. Phys. Solids **48**(1), 175–209 (2000)

X. Tian, Q. Du, Asymptotically compatible schemes and applications to robust discretization of nonlocal models. SIAM J. Numer. Anal. **52**(4), 1641–1665 (2014)

X. Tian, Q. Du, M. Gunzburger, Asymptotically compatible schemes for the approximation of fractional laplacian and related nonlocal diffusion problems on bounded domains. Adv. Comput. Math. **42**(6), 1363–1380 (2016a)

X. Tian, Q. Du, M. Gunzburger, Asymptotically compatible schemes for the approximation of fractional laplacian and related nonlocal diffusion problems on bounded domains. Adv. Comput. Math. **42**(6), 1363–1380 (2016b)

O. Weckner, E. Emmrich, Numerical simulation of the dynamics of a nonlocal, inhomogeneous, infinite bar. J. Comput. Appl. Mech. **6**(2), 311–319 (2005)

G. Zhang, Q. Le, A. Loghin, A. Subramaniyan, F. Bobaru, Validation of a peridynamic model for fatigue cracking. Eng. Fract. Mech. **162**, 76–94 (2016)